NATIONAL ADVISORY COMMITTEE FOR AERONAUTICS

TECHNICAL NOTE 2857

A THEORETICAL METHOD OF ANALYZING THE EFFECTS OF YAW-DAMPER DYNAMICS ON THE STABILITY OF AN AIRCRAFT EQUIPPED WITH A SECOND-ORDER YAW DAMPER

By Albert A. Schy and Ordway B. Gates, Jr.

Langley Aeronautical Laboratory
Langley Field, Va.

NACA

Washington

December 1952

1Q

NATIONAL ADVISORY COMMITTEE FOR AERONAUTICS

TECHNICAL NOTE 2857

A THEORETICAL METHOD OF ANALYZING THE EFFECTS OF YAW-DAMPER DYNAMICS ON THE STABILITY OF AN AIRCRAFT EQUIPPED WITH A SECOND-ORDER YAW DAMPER

By Albert A. Schy and Ordway B. Gates, Jr.

SUMMARY

A method is described for investigating the effects of the dynamic response of an autopilot on the stability of an aircraft-autopilot combination. The method is based on a study of the constant-damping curves obtained in a plane defined by varying two of the autopilot parameters. The dynamics of the autopilot are assumed to be describable by a second-order differential equation. The effects on the system stability of varying the gain, natural frequency, and damping ratio of the automatic damper are investigated, since these parameters determine the dynamic response of the automatic damper.

The method is applied to the analysis of the lateral motion of an airplane equipped with a second-order automatic yaw-rate damper. For any condition of the airplane, an optimum combination of values of autopilot natural frequency and damping ratio are shown to exist for any given gain or required damping. A simple, analytical expression is derived for obtaining a close approximation to these optimum points by ignoring the effects of the aperiodic characteristic modes of the airplane. The assumption that these aperiodic modes may be neglected in considering the effect of the yaw damper on the Dutch roll oscillation is used in all the subsequent analysis. Expressions are derived for the maximum damping obtainable under various conditions. For any given natural frequency and damping ratio of the autopilot, excessive autopilot gain will always cause the autopilot oscillatory mode to become unstable.

Finally, the problem of designing an efficient yaw damper which will improve the damping of the Dutch roll oscillation for various flight conditions of an airplane is considered. A simple method of design is illustrated by applying it to three flight conditions of an airplane.

Calculated motions, based on the assumption of three degrees of freedom for the lateral airplane motion, are presented. They agree

with the results obtained from the constant-damping-curve analysis when the aperiodic airplane modes are neglected.

INTRODUCTION

Recently, a great deal of interest has been shown in the use of automatic stabilization devices for improving the damping of the lateral (Dutch roll) oscillation of aircraft designed to travel at transonic and supersonic speeds. The analyses of such automatic stabilization systems may be divided into two classes. In one kind of analysis the effects of various types of autopilots on aircraft stability are considered, and usually the autopilot is assumed to be an idealized system with no lags. In the other kind of analysis the effects of the dynamic response of a particular type of stabilization system on the stability of the aircraft-autopilot combination are considered.

Some investigations of the effects of various types of idealized autopilots on airplane lateral stability are reported in references 1 to 3. References 1 and 2 are theoretical analyses, whereas in reference 3 experimental results are compared with theoretically predicted effects.

Analyses of the second kind, in which the effects of certain types of dynamic response in a given stabilization system are considered, have involved various approaches to the problem of determining the stability of the complete system. The well-known frequency-response analysis has been used in many papers (for example, in ref. 4). Applications of Nyquist's stability criterion, which was originally developed for feedback amplifiers, have also been used. For example, in reference 5 Nyquist's criterion is extended to systems with constant time lag in the feedback circuit.

When the conditions which will insure a given amount of stability, rather than just neutral stability, are sought, the use of constant-damping curves has been found convenient. The method is described in reference 6, and an example of its application is furnished by reference 7. In reference 8 a semigraphical method is developed for obtaining the conditions which insure neutral stability of an airplane-autopilot system when a constant time lag in the autopilot is assumed; also, a procedure is indicated for using the method of constant-damping curves to determine the conditions which insure a given amount of damping. This method is described in detail in reference 9.

In the present paper the constant-damping-curve analysis is applied to an airplane-autopilot system in which the autopilot dynamics are represented by a second-order differential equation. Generally, the

actual frequency response of most autopilots (especially yaw dampers) is better approximated when a second-order differential equation is used to describe the dynamic characteristics of the autopilot than when the constant-time-lag response is assumed. Physically, this assumption implies that the autopilot may be represented as a damped oscillatory system. The present paper examines in some detail the effects on the airplane-autopilot stability of variations in the gain, natural frequency, and damping ratio of the autopilot.

SYMBOLS

A, B coefficients of second-order differential equation for autopilot dynamics (see eq. (1))

b wing span, ft

$$C_1 = \frac{-V^2 C_{n_\delta}}{2b^2\mu_b\left(K_Z^2 - \frac{K_{XZ}^2}{K_X^2}\right)}$$

C_L trim lift coefficient, $W \cos \gamma / qS$

C_l rolling-moment coefficient, Rolling moment/qSb

C_n yawing-moment coefficient, Yawing moment/qSb

C_Y lateral-force coefficient, Lateral force/qS

$$C_{l_\beta} = \frac{\partial C_l}{\partial \beta} \qquad C_{Y_\beta} = \frac{\partial C_Y}{\partial \beta} \qquad C_{n_\beta} = \frac{\partial C_n}{\partial \beta}$$

$$C_{l_p} = \frac{\partial C_l}{\partial \frac{pb}{2V}} \qquad C_{Y_p} = \frac{\partial C_Y}{\partial \frac{pb}{2V}} \qquad C_{n_p} = \frac{\partial C_n}{\partial \frac{pb}{2V}}$$

$$C_{l_r} = \frac{\partial C_l}{\partial \frac{rb}{2V}} \qquad C_{Y_r} = \frac{\partial C_Y}{\partial \frac{rb}{2V}} \qquad C_{n_r} = \frac{\partial C_n}{\partial \frac{rb}{2V}}$$

$$C_{n_\delta} = \frac{\partial C_n}{\partial \delta}$$

D time-derivative operator, d/dt

$F(D)$ characteristic polynomial of airplane-autopilot system

$F_o(D)$ characteristic polynomial of airplane alone

$f_n(R) = \frac{1}{n!}\frac{d^nF(R)}{dR^n}$

$i = \sqrt{-1}$

K gearing ratio of second-order autopilot, deg/deg/sec

K_o gearing ratio required for an ideal no-lag rate damper to provide a given amount of damping, deg/deg/sec

K_X nondimensional radius of gyration in roll about longitudinal stability axis

K_Z nondimensional radius of gyration in yaw about normal stability axis

K_{XZ} nondimensional product-of-inertia parameter

m mass of airplane, slugs

n an integer

P, Q coefficients of a quadratic factor of characteristic equation of airplane-autopilot system

P_o, Q_o coefficients of Dutch roll quadratic (see eq. (10))

$p = D\phi$

q dynamic pressure, $\frac{1}{2}\rho V^2$, lb/sq ft

R real part of characteristic root, sec^{-1}

$r = D\psi$

S wing area, sq ft

$T_{1/2}$ time for amplitude of oscillation to damp to one-half its original value, sec

t time, sec

V	steady-state velocity, ft/sec
W	weight of airplane, lb
β	angle of sideslip, radians unless otherwise specified
γ	flight-path angle, radians
δ	deflection of control surface, deg or radians
ζ	damping ratio of second-order autopilot
μ_b	relative-density factor, $m/\rho Sb$
ρ	air density, slugs/cu ft
ϕ	angle of bank, radians unless otherwise specified
ψ	angle of yaw, radians unless otherwise specified
ω	angular frequency (always referred to simply as "frequency"), radians/sec
ω_A	frequency of Dutch roll oscillation, radians/sec
ω_o	natural frequency of second-order autopilot, radians/sec
$[\,]_A(D)$	transfer function of airplane
$[\,]_P(D)$	transfer function of autopilot

Subscripts:

cr	critical
max	maximum

ANALYSIS

Preliminary Discussion

The dynamics of an autopilot used for aircraft stabilization can often be represented by a differential equation of the type

$$D^2\delta + AD\delta + B\delta = KBX \qquad (1)$$

Here δ is the deflection of the control surface actuated by the autopilot, and X is the component of airplane motion to which the autopilot is sensitive. In general, X may be any combination of the airplane degrees of freedom or their time derivatives, or both. When B is positive, as it must be for stable autopilots, let $A = 2\zeta\omega_o$ and $B = \omega_o^2$. Then equation (1) becomes

$$D^2\delta + 2\zeta\omega_o D\delta + \omega_o^2\delta = K\omega_o^2 X \qquad (2)$$

Although A and B are often more convenient to use for purposes of analysis, the equivalent parameters ζ and ω_o are more meaningful physically. Most of the results of this paper will therefore be presented in terms of these parameters. The parameter ω_o is the natural (undamped) frequency of the autopilot system and the parameter ζ is the damping ratio, that is, the ratio of the actual damping of the system to the critical damping. The parameter K which appears in equations (1) and (2) is variously called the amplification factor, the gain, or the gearing ratio. An autopilot which may be represented by equation (1) or (2) is often called a second-order autopilot, since the dynamics of the autopilot are represented by an expression involving time derivatives of the control deflection up to and including second-order derivatives.

The coefficients of the characteristic equation of an airplane equipped with a second-order autopilot are functions of the stability derivatives and mass characteristics of the airplane and of the three autopilot parameters K, ω_o, and ζ (or K, A, and B). These coefficients are often called the stability coefficients. If the stability derivatives and mass characteristics of the airplane are known for a given flight condition, and if one of the autopilot parameters is assigned some reasonable value, then the stability coefficients of the airplane-autopilot system are functions of the remaining two autopilot parameters only. Curves of constant damping of the characteristic modes of the total system may therefore be drawn in the plane defined by considering these two parameters as independent variables. Methods of obtaining such curves, with particular application to oscillatory modes, are discussed in references 6 and 7. From an examination of the constant-damping curves the ranges of values of the two independent autopilot parameters which will provide a given amount of damping to the oscillatory modes of the airplane-autopilot system can be determined. Moreover, a detailed study of these constant-damping curves yields a considerable amount of insight into some of the fundamental properties of the motions of airplanes equipped with second-order automatic stabilization systems.

Application to Second-Order Yaw-Rate Damper

Equations of motion.- The method has been applied to the analysis of the effect of a yaw-rate damper on the lateral stability of an airplane. When the dimensional time-derivative operator is used, the lateral equations of motion are

$$2\mu_b D\beta - \frac{V}{b} C_{Y_\beta}\beta + 2\mu_b D\psi - \frac{V}{b} C_L\phi = \frac{V}{b} C_Y \tag{3}$$

$$- \frac{V^2}{b^2} C_{n_\beta}\beta + 2\mu_b K_Z{}^2 D^2\psi - \frac{1}{2}\frac{V}{b} C_{n_r} D\psi + 2\mu_b K_{XZ} D^2\phi - \frac{1}{2}\frac{V}{b} C_{n_p} D\phi =$$

$$\frac{V^2}{b^2} C_{n_\delta}\delta - \frac{V^2}{b^2} C_n \tag{4}$$

$$- \frac{V^2}{b^2} C_{l_\beta}\beta + 2\mu_b K_{XZ} D^2\psi - \frac{1}{2}\frac{V}{b} C_{l_r} D\psi + 2\mu_b K_X{}^2 D^2\phi - \frac{1}{2}\frac{V}{b} C_{l_p} D\phi = \frac{V^2}{b^2} C_l \tag{5}$$

In these equations the assumptions are made that $C_{Y_p} = C_{Y_r} = \gamma = 0$ and that the only result of the control deflection δ is a yawing moment. The equation of motion of the yaw-rate damper, written in the form of equation (2), is

$$D^2\delta + 2\zeta\omega_o D\delta + \omega_o{}^2\delta = K\omega_o{}^2 D\psi \tag{6}$$

The complete characteristic equation for the equations of motion (3) to (6) is a sixth-degree equation. In fact, if $F_o(D)$ be the usual fourth-order characteristic polynomial for the lateral degrees of freedom described by equations (3) to (5) (see ref. 2), then the complete characteristic equation for the airplane-autopilot combination is

$$F(D) = \left(D^2 + 2\zeta\omega_o D + \omega_o{}^2\right)F_o(D) - \frac{V^2}{b^2} C_{n_\delta} K\omega_o{}^2 \left[\left(2\mu_b D - \frac{V}{b} C_{Y_\beta}\right)\left(2\mu_b K_X{}^2 D^2 - \frac{1}{2}\frac{V}{b} C_{l_p} D\right) - \frac{V^3}{b^3} C_L C_{l_\beta}\right]$$

$$= 0 \tag{7}$$

The characteristic modes obtained from this equation are usually two oscillations and two aperiodic modes. In most cases the two aperiodic modes and one of the oscillations may be associated with the lateral motion of the airplane, whereas the second oscillation may be associated with the motion of the autopilot system.

Choice of variable autopilot parameters for constant-damping curves.- If all the parameters in equations (3) to (5) are known for an airplane in a given flight condition, the effects of K, ω_o, and ζ on the lateral oscillatory stability of the combined system can be determined by varying these parameters in equation (7), as is shown in appendix A. One of these parameters must be fixed if the stability boundaries are to be plotted in a plane as described in appendix A, and therefore the relative convenience of fixing each of the three parameters should be considered. Since the dynamic characteristics of the autopilot may be expressed in terms of its frequency response, a study of the effects of the three autopilot parameters on this frequency response should provide some insight into the question of which two parameters should be varied simultaneously.

The transfer function of the stabilizing autopilot may be obtained from equation (6):

$$\left[\delta/D\bar{\psi}\right]_P(D) = \frac{K\omega_o^2}{D^2 + 2\zeta\omega_o D + \omega_o^2} \tag{8}$$

Therefore, the expression for the autopilot frequency response is

$$\left[\delta/D\bar{\psi}\right]_P(i\omega) = \frac{K}{1 - \frac{\omega^2}{\omega_o^2} + 2i\zeta\frac{\omega}{\omega_o}} \equiv R_P(\omega)e^{i\theta_P(\omega)} \tag{9}$$

The frequency response of the autopilot is obtained from equation (9) by plotting the amplitude $R_P(\omega)$ and phase angle $\theta_P(\omega)$ of the complex number $\left[\delta/D\bar{\psi}\right]_P(i\omega)$ against ω. The phase angle is independent of K, whereas the magnitude at any value of ω is proportional to K. Thus the phase-angle curve and the shape of the magnitude curve both depend only on ζ and ω_o, and the gearing ratio simply acts as an amplification factor on the magnitude curve. From this point of view, it would seem desirable to select reasonable values of K and allow ζ and ω_o to be the variable parameters in equation (7). A study of the stability boundaries in the $\zeta\omega_o$-plane would then show the effect of

varying the shape of the autopilot frequency response on the stability of the total system, whereas the variation of K would show the effect of varying the amplification factor. The stability boundaries were therefore first calculated in the $\zeta\omega_o$-plane, and some of the effects of varying K on these curves were investigated.

Since the gearing ratio K is in many respects the most important parameter determining the stability of the total system, stability boundaries were also obtained in the $K\omega_o$-plane for fixed values of ζ. This method of plotting the stability boundaries has two distinct advantages. First, the two most important parameters, K and ω_o, are allowed to vary. Second, the fixed parameter ζ is known to be between 0 and 1 for stable oscillatory autopilot systems; therefore, the effect of varying ζ on the stability boundaries in the $K\omega_o$-plane can be determined fairly easily by choosing several values of ζ which will span this range.

Constant-damping curves with gearing ratio fixed; three degrees of freedom.- In order to investigate the effect of the second-order yaw damper on the stability of the system, values of the airplane parameters were inserted into equations (3) to (5) to correspond to a cruising flight condition for the airplane described in table I. The Dutch roll oscillation for this flight condition has a period of 1.30 seconds and $T_{1/2}$ of 2.60 seconds.

In order to investigate the type of constant-damping curve which appears in the $\zeta\omega_o$-plane (or AB-plane) for constant K, a value of K was chosen which would give good damping if used in a perfect proportional yaw damper that has no inertia or damping. The value K = 0.086 degree of rudder deflection per degree per second of yawing velocity was chosen, which would make $T_{1/2}$ of the Dutch roll oscillation equal to 0.75 second. The constant-damping curves in the AB-plane were then drawn for this value of K by using the equations given in appendix A, and are shown in figures 1 to 5. The frequencies of the modes on a given curve vary from zero to infinity, and typical values are shown on the individual curves.

As pointed out in appendix A, it is simpler to obtain the curves first in terms of A and B and then substitute the more significant parameters ζ and ω_o. However, for a preliminary investigation of the general types of curves and the manner in which they change as R and ω (the damping and frequency parameters) are varied, continued use of the AB-plane is more convenient because negative values of B may be considered, whereas the parameters ζ and ω_o have an obvious physical significance only for positive values of B. For this reason, the typical curves of figures 1 to 5 are drawn in the AB-plane. These figures are presented and discussed primarily to familiarize the reader

with the general types of curves which occur, so that the later comparison of the curves in the $\zeta\omega_o$-plane will not be too confusing. The practically significant portions of the curves are essentially the same in either plane.

Figure 1 presents the zero-damping curve, which is continuous and crosses itself to form a loop. The loop has no practical significance, since it merely defines the region of autopilot parameters for which there are two unstable oscillations. The hatch marks indicate the boundary of the region in which all modes are stable. In all cases the $B = 0$ axis is the boundary at which an aperiodic mode becomes unstable.

The curve of greatest practical importance is that defined by the damping of the airplane without the autopilot; that is, the curve for $T_{1/2} = 2.60$ seconds. This curve, shown in figure 2, is discontinuous. When ω approaches the airplane frequency (the frequency of the Dutch roll oscillation of the airplane alone), both A and B become infinite in magnitude. These infinities are caused by the vanishing of a factor in the denominator of the expressions for A and B. At the airplane frequency a new branch of the constant-damping curve is started. The region in the AB-plane in which there are no oscillatory modes that have less damping than the airplane alone (indicated by hatch marks) is bounded by this new branch of the curve. The dashed line shows the value $B = Q_o = 23.84$, where Q_o is the constant coefficient of the Dutch roll quadratic, which is written as $D^2 + P_oD + Q_o$. The significance of this value will be discussed subsequently.

Figure 3 shows a typical curve for a damping somewhat greater than that of the airplane alone. It has two points of discontinuity and three branches. Thus, the airplane-damping curve shown in figure 2 is a critical curve, separating the continuous curves for less damping from the doubly discontinuous curves for greater damping. The two critical values of ω are very close, so that the branch of the curve in the negative-B region corresponds to a very small range of ω. This branch of the curve is of academic interest only. The part of the curve in figure 3 which forms the significant boundary is again the curve in the upper right quadrant of the plane, defining a region of better damping indicated by hatch marks.

The curve in figure 4 is for $T_{1/2} = 0.75$ second, the damping which the airplane-autopilot oscillation would have if the autopilot had no lags. This curve has another branch at large negative values of B and negative A, but this branch is not shown because, as has been mentioned, it is of academic importance only. (It should be noted that the significant portions of all these discontinuous curves start at values of ω near the airplane frequency.) The curve for $T_{1/2} = 0.75$ second also represents a critical damping value, since

for larger values of damping the curves again become continuous and form loops, as shown in figure 5 for $T_{1/2} = 0.60$ second. In the following discussion the damping corresponding to $T_{1/2} = 0.75$ second and the associated constant-damping curve will be called the critical damping and critical curve.

These curves will be discussed in greater detail. For the present it will suffice to note that, for any gearing ratio, greater damping can be provided by a second-order autopilot than could be provided by a perfect proportional autopilot with the same gearing ratio, provided that the proper values of ζ and ω_o are chosen from a closed-loop region of the type shown in figure 5.

Equivalent-oscillator concept.- Appendix A shows that, in determining the effect of the yaw damper on the stability of the Dutch roll oscillation, the airplane is represented by an equivalent oscillator whose period and damping are those of the Dutch roll oscillation. Explicitly, the assumption is made that the three-degree-of-freedom equations of motion of the airplane, given by equations (3) to (5), may be replaced by the single equation of motion

$$2\mu_b\left(K_Z^2 - \frac{K_{XZ}^2}{K_X^2}\right)\left(D^2\psi + P_oD\psi + Q_o\psi\right) - \frac{V^2}{b^2}C_{n_\delta}\delta = \frac{V^2}{b^2}C_n \qquad (10)$$

The physical interpretation of this assumption is that the effect of the aperiodic modes on the Dutch roll stability is small. The quadratic equation $D^2 + P_oD + Q_o = 0$ yields the complex characteristic root corresponding to the Dutch roll oscillatory mode.

The analysis is greatly simplified by this equivalent-oscillator concept, and it will be seen that this simplified analysis gives adequate results. Except where otherwise specified, the equivalent oscillator is assumed to represent the airplane in all the subsequent discussions. The curves in figures 1 to 5, obtained from the three-degree-of-freedom analysis, were drawn primarily as a check of the accuracy of the equivalent-oscillator approximation.

In figure 6 the constant-damping curves calculated by the equivalent-oscillator analysis for representative values of damping are presented in the $\zeta\omega_o$-plane. In interpreting these curves it is essential to remember that two oscillations are present for most of the significant points in the $\zeta\omega_o$-plane. One of these oscillations may generally be associated with the airplane and the other with the autopilot. Therefore, at every point in the most significant regions of the $\zeta\omega_o$-plane two damping curves must cross each other.

All the curves previously obtained from the three-degree-of-freedom analysis are presented in figure 6, and in addition the boundary of equal roots and the curve for $T_{1/2} = 0.38$ second are shown. Each of the constant-damping curves starts on the boundary of equal roots at $\omega = 0$. Before the general discussion of figure 6 is presented, the significance of the curve for $T_{1/2} = 0.38$ second will be explained.

Maximum damping with fixed gearing ratio.- As mentioned previously, the constant-damping curves for higher damping than the critical damping are continuous and form loops defining the regions which insure greater damping. Since the loops become smaller for larger values of damping, it is reasonable to assume that for some value of damping the loop will become vanishingly small - only a cusp in the curve (see ref. 9). This curve then corresponds to the maximum damping which can be obtained for the Dutch roll oscillation with a second-order yaw-rate damper for the given gearing ratio. Thus the cusp point may be considered the optimum point in the $\zeta\omega_o$-plane for a given gearing ratio, and this point determines the shape of the autopilot frequency response which will give the highest damping to the Dutch roll oscillation for a given amplification factor K.

These optimum points may be obtained by a rather simple algebraic analysis because they correspond to a double oscillatory root of the characteristic equation, which is a quartic equation when the equivalent-oscillator concept is used. The derivation of the optimum-point characteristics is presented in appendix B. The damping and frequency of the double oscillatory mode are assumed to be given by the characteristic equation

$$(D^2 + PD + Q)^2 = 0 \tag{11}$$

As shown in appendix B, the value of Q may be obtained by solving the quadratic equation, for a given gearing ratio,

$$\left(1 + \frac{C_1 K}{P_o \pm 2\sqrt{Q_o}}\right)Q^2 - 2Q_oQ + Q_o^2 = 0 \tag{12}$$

For positive values of K the larger real root in equation (12) is used. With this value for Q, P may be obtained from the expression

$$P = \frac{(P_o + C_1 K)Q^2 - P_o Q_o^2}{2Q_o(Q - Q_o)} \tag{13}$$

These values of P and Q, when used in equation (11), give the characteristic root (and therefore the period and damping) corresponding to the best-damped Dutch roll motion obtainable with the given gearing ratio. In order to find the autopilot parameters A and B (or ζ and ω_o) which yield this maximum damping, these values of P and Q are substituted into the following expressions for A and B:

$$A = 2P - P_o \tag{14}$$

$$B = \frac{Q^2}{Q_o} \tag{15}$$

The maximum damping for the airplane under discussion for $K = 0.086$ deg/deg/sec was obtained in this manner and was found to correspond to $T_{1/2} = 0.38$ second. As can be seen from figure 6, this curve does have a cusp at the optimum point in the $\zeta\omega_o$-plane.

Since the high-damping curves in the three-degree-of-freedom analysis also form loops, the same type of analysis can be used to obtain the cusp point in the $\zeta\omega_o$-plane. The calculation of the maximum damping would be much more complicated, however, for the three-degree-of-freedom case. To show that the maximum damping as calculated by the equivalent-oscillator analysis is an adequate approximation to the maximum damping for the complete airplane, the curve for $T_{1/2} = 0.38$ second was drawn for the three-degree-of-freedom case also.

The comparison of the curves for $T_{1/2} = 0.38$ second for the two cases is shown in figure 7. In this figure the significant portions of other typical damping curves are also shown. For practical purposes, the equivalent-oscillator analysis is an adequate approximation to the three-degree-of-freedom analysis in determining the required constant-damping curves, including the maximum-damping point. It might also be noted that the critical damping is not exactly the same in the two cases ($T_{1/2} = 0.75$ second for the three-degree-of-freedom case and $T_{1/2} = 0.73$ second for the equivalent one-degree-of-freedom case).

Discussion and interpretation of damping boundaries in $\zeta\omega_o$-plane.- Figure 7 shows that there is little change in the stability boundaries when the lateral motion of the airplane is represented by the equivalent oscillator. This result means that the real characteristic modes of the lateral motion can be neglected in calculating the effect of the automatic yaw damper on the Dutch roll oscillation. The only fundamental

difference occurs in the airplane-damping curve, $T_{1/2} = 2.60$ seconds. For the equivalent oscillator, this curve is discontinuous at a value of ω_o equal to the airplane frequency, 4.8 radians per second. The slope of the curve becomes infinite at this value of ω_o, and the portion of the curve bounding the higher-damping region begins here at $\zeta = \infty$. In the three-degree-of-freedom analysis, the curve for $T_{1/2} = 2.60$ seconds has a slope which becomes very large at $\omega_o = 4.8$ radians per second but remains finite. Thus the difference in the curves is negligible for practical purposes. Since the significant portion of the airplane-damping curve begins at $\omega_o = 4.8$ radians per second for any positive gearing ratio, the damping of the equivalent oscillator cannot be improved with a positively geared yaw-rate damper which has a natural frequency less than the frequency of the oscillator itself. Figure 7 shows that for practical purposes the same statement can be made for the actual airplane.

Certain general effects of varying the autopilot damping and natural frequency on the stability of the system may be observed in figures 6 and 7. The area of interest is the roughly rectangular region indicated by the hatch marks in figure 2 in the AB-plane, in which both oscillatory modes have more damping than the airplane alone. The value of B indicated by the dashed line in figure 2 corresponds to the airplane frequency ($\omega_o = 4.8$ radians per second). If ζ is fixed at any positive value and ω_o is increased, figure 6 indicates that the system damping increases to a maximum value at some value of ω_o and then drops off, approaching the critical damping as ω_o approaches infinity. Similarly, at any fixed natural frequency greater than the Dutch roll frequency, if the value of ζ is increased from zero the damping reaches a maximum at some value of ζ and then drops off, approaching the airplane damping as ζ approaches infinity. Thus, for fixed ζ there is an optimum ω_o, and for fixed ω_o an optimum ζ. The best of all these points is the maximum-damping point, which is obtained by the simple calculation previously described.

Importance of oscillation frequencies in interpreting constant-damping curves.- From stability considerations alone, the regions defined by the hatch-marked portions of the curves shown in figures 1 to 5 determine the values of autopilot parameters which guarantee at least the indicated amount of damping. However, points may be chosen outside a given region which still seem to give an airplane motion that is as well-damped as that for points in the region. For example, figure 8 shows the motions obtained with autopilots having the characteristics defined by points 1, 2, and 3 in figure 6. All motions shown in this paper were obtained from a Reeves Electronic Analog Computer, by use of the three-degree-of-freedom equations of motion. The fact that these motions check

the predictions made from the equivalent-oscillator stability boundaries confirms the adequacy of the equivalent-oscillator analysis.

Points 2 and 3 are on the good portion (loop) of the curve for $T_{1/2} = 0.60$ second, but point 1 is on the intersection of the curves for $T_{1/2} = 0.60$ second and $T_{1/2} = 2.60$ seconds and is outside the good region defined by the loop. However, the actual airplane motions, represented by the sideslip and roll motions in figure 8, are very similar for all three autopilots, and the lightly damped mode is important only in the rudder motion for the case corresponding to point 1 (fig. 8(a)). Actually, the effect of the lightly damped mode can be seen in the sideslip motion of figure 8(a), but it is almost negligible. Although point 1 in figure 6 corresponds to $T_{1/2} = 2.60$ seconds, as far as the airplane motion is concerned this autopilot would seem to give as good damping as autopilots whose characteristics fall in the loop of $T_{1/2} = 0.60$ second.

In order to understand why the lightly damped mode corresponding to point 1 in figure 6 has practically no effect on the airplane motion, the frequencies of the modes which are predicted at this point must be considered. Since for the most significant points in the $\zeta\omega_o$-plane there must be two characteristic oscillations, each of these points is actually a crossing point of two constant-damping curves, as can be seen for point 1 in figure 6. The general trends of the frequencies along the damping curves are shown in figures 1 to 5. Along the final portion of each curve (that is, the portion which approaches the $\zeta = 0$ axis), the frequencies correspond to the autopilot frequency. At point 1 in figure 6 the mode on the curve for $T_{1/2} = 2.60$ seconds has a frequency $\omega \approx 10$ radians per second, a value which corresponds to the autopilot frequency (as can be seen from fig. 2), whereas the better-damped mode is the airplane mode with $\omega \approx 5$ radians per second (see fig. 5). Since the frequency of the autopilot mode is approximately twice that of the airplane mode, the effect of the corresponding lightly damped rudder oscillation on the airplane motion is small, for the airplane cannot follow such rapid oscillations.

Consideration of the frequencies which occur at points along the damping curves is thus seen to be important in attempting to predict the type of motion which would be obtained with autopilots whose characteristics are determined by these points. This frequency effect is brought out even more strongly by figure 9, which shows the motions corresponding to points 4 and 5 in figure 6. In this case both points are on the zero-damping curve. At point 5 both modes have approximately the same frequency. However, at point 4 the autopilot frequency is the neutrally damped one, with $\omega \approx 13.5$ radians per second, and the airplane mode lies on one of the well-damped loop curves, which crosses the curve for $T_{1/2} = \infty$ at point 4. The motions shown give the results predicted

by the analysis. As shown in figure 9(a), corresponding to point 4, the neutrally damped high-frequency rudder motion has little effect on the well-damped airplane motion. On the other hand, for point 5 the effect of the neutrally damped mode, which is close to the natural airplane frequency, is the dominant neutrally damped airplane oscillation shown in figure 9(b). Autopilots which cause very poorly damped control motions, however, would be unsatisfactory from a practical point of view even if their effect on the airplane damping were satisfactory.

Effect of varying K on curves in $\zeta\omega_o$-plane.- The effect of gearing ratio may be obtained by considering the effect of varying K on the curves in the $\zeta\omega_o$-plane. By using the equivalent-oscillator analysis, the critical damping is found to be $R_{cr} = -\frac{1}{2}(P_o + C_1K)$. Since the airplane damping is $-\frac{1}{2}P_o$, the critical damping becomes the airplane damping as K vanishes. This result is, of course, necessary, since zero gearing ratio implies no autopilot. As K is made smaller, the whole set of loop curves in figure 6 tends to move to the left, since the critical curve approaches the airplane damping curve. Conversely, as K increases, these curves move to the right. Also, the loop corresponding to any given damping larger than the critical damping must expand as K increases, since the given damping comes closer to the critical damping. Therefore the given loop approaches the infinite loop asymptotic to the critical-damping curve. Physically, this result simply means that as the gearing ratio is increased there is a larger range of values of ζ and ω_o for which a given damping larger than the critical damping may be obtained.

A clearer idea of the way in which the set of loop curves moves in the $\zeta\omega_o$-plane as K varies is obtained by investigating the variation of the maximum-damping point as K varies. The position of the maximum-damping point is itself important, because it is the optimum combination of ζ and ω_o for any value of K; but, also, since this point is a kernel which is surrounded by all the loops, the motion of this point gives a clearer idea of the motion of any loop as K varies. The desired variation may be easily obtained by inserting values of K into equations (12) and (13), and using the resulting values of P and Q in equations (14) and (15). However, a simpler and clearer method is shown to be possible in appendix B, wherein a value of damping is assumed and solutions are found for the values of K, A, B, and Q which will make this the maximum damping. This procedure clearly gives the smallest magnitude of K with which the desired damping may be obtained with the second-order automatic yaw damper, and the associated values of A and B then may be considered as "optimum" values for the given airplane and desired damping. In this method equation (13) is replaced by

$$P = -2R = \frac{1.386}{T_{1/2}} \tag{16}$$

where R and $T_{1/2}$ correspond to the desired damping. Equation (14) then gives A immediately, and Q may be obtained from the expression

$$Q = Q_o \pm \sqrt{Q_o}(P - P_o) \tag{17}$$

Equation (17) will give two values of Q, one greater than Q_o and the other less than Q_o. By using these values in equation (15), the corresponding values of B are obtained, and from equation (13):

$$K = \frac{2PQ - P_oB - AQ_o}{C_1B} \tag{18}$$

The smaller value of Q obtained from equation (17) gives a value of B corresponding to a value of ω_o lower than the airplane frequency and results in a negative K. The larger value of Q gives a value of ω_o higher than the airplane frequency and positive gearing. Figures 10 and 11 show the variation of the optimum points. Figure 10 shows the curve on which the points lie in the $\zeta\omega_o$-plane. Figure 11 shows the gearing necessary to obtain any given damping as the maximum damping (when the autopilot characteristics are the optimum ones for that gearing).

The point corresponding to K = 0 on each curve is significant only as a limiting point, since zero gearing implies no autopilot. Since the double oscillatory mode corresponding to the maximum damping must approach the Dutch roll mode as K approaches zero, the optimum point in the $\zeta\omega_o$-plane approaches the values corresponding to the Dutch roll mode. Increased damping of the system can be obtained with either positive or negative gearing. The positive-K branch of the locus of optimum points given in figure 10 lies in the range of values of ω_o higher than the airplane frequency. Thus, as mentioned previously, second-order yaw dampers with positive gearing must have a value of ω_o higher than the airplane frequency in order to improve the damping. Also, the variation of the optimum points on the positive-K branch of figure 10 shows that, if increased damping from the autopilot is sought by increasing the gearing ratio, the natural frequency and damping ratio of the autopilot should generally be increased simultaneously. This fact can be of considerable practical importance, as will be brought out more clearly in subsequent discussion.

Comparison of advantages of positive and negative gearing.- If negative gearings are used, ω_o values lower than the airplane frequency must be used in order to improve the damping. The possibility of using

a negatively (reverse) geared second-order rate autopilot to improve the damping seems rather surprising, since for a perfect proportional rate autopilot, reverse gearing would simply decrease the effective C_{n_r} and therefore decrease the damping. The use of reverse gearing is made possible by the phase relations introduced between the airplane and rudder motions by the dynamics of the second-order autopilot. Actually, this possibility is no more surprising than the fact that this type of autopilot will improve the damping with positive gearing only when the autopilot natural frequency is greater than the airplane frequency. Clearly, this restriction arises from the same type of phase-relation requirement.

The use of a negatively geared yaw damper would seem advantageous because of its properties in a steady turn. For constant yawing velocity the negatively geared yaw damper deflects the rudder in a direction to maintain the turn, whereas the positively geared yaw damper must be overridden, either by the pilot or by the boost system. However, certain objections to the use of negative gearing in an automatic damper for use with an airplane actually make such use impractical.

The main objection to the use of negative gearing is based on the fact that the equivalent oscillator represents the airplane only in a given flight condition. At different flight conditions the characteristic airplane oscillation has different values of damping and frequency; therefore, the airplane is represented by a different equivalent oscillator at each flight condition. To design an automatic damper for one flight condition only is impractical, since this automatic damper may have a harmful effect on the damping at some other flight condition. Autopilot characteristics must therefore be obtained by some compromise method which will improve any practical flight condition. Now, it can be shown that the regions of improved damping in the $\zeta\omega_o$-plane for negative values of K are loops resembling a reflection in the $A = 0$ axis of the unstable loop shown in figure 1. These loops must lie in a relatively narrow range of ω_o values, since they are confined to values of ω_o lower than the airplane frequency. Moreover, for a given magnitude of gearing ratio, the loop for any damping is much smaller for negative K than for positive K. Figure 11 shows that the loops for negative values of K break down at much smaller values of damping than the loops for positive values of K of the same magnitude. If these small loops in the $\zeta\omega_o$-plane are drawn for a desired amount of damping for two extreme flight conditions with different natural frequencies, the possibility of their intersecting in a region of the $\zeta\omega_o$-plane which would give the desired damping to both flight conditions is relatively small.

For positive gearing, on the other hand, improved damping can be obtained up to the critical damping for an infinite range of ω_o starting at a value of ω_o somewhat greater than the natural airplane frequency

in the particular flight condition. There is, therefore, an infinite range of ω_o values which will insure at least the critical damping for any number of flight conditions. The minimum value of ω_o necessary is somewhat greater than the highest natural frequency of any of the possible flight conditions of the airplane.

Maximum damping for any gearing ratio.- The highest maximum damping and the corresponding value of K can be obtained by determining where the modes corresponding to the optimum points in figures 10 and 11 become nonoscillatory. This condition will occur for $P^2 = 4Q$. By using this condition in equation (17), where the positive sign corresponds to positive K and the negative sign to negative K, the following expressions are obtained:

$$P_{max} = 2\sqrt{Q_o}\left(\sqrt{2 - \frac{P_o}{\sqrt{Q_o}}} + 1\right) \qquad (K > 0) \qquad (19)$$

$$P_{max} = 2\sqrt{Q_o}\left(\sqrt{2 + \frac{P_o}{\sqrt{Q_o}}} - 1\right) \qquad (K < 0) \qquad (20)$$

Since P_o is small for lightly damped airplanes, the positive gearing ratio gives a higher value. For example, for $P_o = 0$, equation (19) gives a value approximately six times as large as equation (20). Actually, these limiting values for the damping are of only academic interest as far as application to the airplane is concerned, since they are so large as to be far above any required damping.

Constant-damping curves in $K\omega_o$-plane with damping ratio fixed.- In order to obtain a more complete picture of the effect of varying gearing ratio on the stability of the system, constant-damping curves were obtained in the $K\omega_o$-plane with ζ fixed. As shown in appendix A, it is necessary to solve a quadratic equation for the ω_o values, which may then be substituted into an expression for K, as follows:

$$\left(Q_o - R^2 - \omega^2\right)\omega_o^2 - 2\zeta\omega_o\left(P_o + 2R\right)\left(\omega^2 + R^2\right) + \omega^4 -$$

$$\left(Q_o + 2P_oR + 2R^2\right)\left(\omega^2 + R^2\right) = 0 \qquad (21a)$$

$$K = \frac{1}{C_1\omega_o^2}\left\{\left(2\zeta\omega_o + P_o + 4R\right)\omega^2 - \right.$$

$$\left.\left[\left(P_o + 2R\right)\omega_o^2 + 2\zeta\omega_o\left(Q_o + P_oR + 3R^2\right) + R\left(2Q_o + 3P_oR + 4R^2\right)\right]\right\} \tag{21b}$$

For the first calculations, $\zeta = 0.3$ was assumed as a reasonable value of damping ratio for the autopilot. A set of curves was obtained for this value of ζ. The effect of varying ζ on the curves in the $K\omega_o$-plane was then investigated by obtaining several typical curves for $\zeta = 0.6$ and $\zeta = 0.9$.

The zero-damping curve for $\zeta = 0.3$ (shown in fig. 12) indicates that better-than-neutral damping can be obtained for any value of ω_o and for positive or negative gearing. This is true for any damping up to the airplane damping. The boundaries for less than the airplane damping are of no practical interest, however, and figure 12 is presented only for completeness.

Figure 13 shows the airplane damping boundary, which is a simple, continuous curve. This curve alone does not indicate clearly the region that defines points which give better damping than that for the airplane without yaw damper. However, the axis $K = 0$ must be part of the boundary also, since $K = 0$ implies no autopilot, which means that the airplane has its original damping. In order to verify that the region defined by the hatching in figure 13 is the good region, a curve was drawn for a slightly greater damping $\left(T_{1/2} = 2.50 \text{ seconds}\right)$. This curve is shown in figure 14 and confirms the fact that the region insuring damping greater than that of the airplane is as shown in figure 13.

The results of figure 13 confirm several of the previous conclusions concerning negative gearing which were obtained from figures 10 and 11. A relatively small region is present in the $K\omega_o$-plane in which improved damping can be obtained with negative K, and this region is confined to frequencies less than the airplane frequency.

Figure 14 shows that the regions of negative K which will give improved damping are loops in the $K\omega_o$-plane. Thus, the maximum damping for negative K may be obtained from the cusp point corresponding to the breakdown of these loops for any values of ζ. Since ζ is constant, a particularly simple expression can be obtained for R_{max}. If ζ and ω_o are used instead of A and B, equations (14) and (15) may be used in equation (17), and the result is

$$\omega_o = \frac{\sqrt{Q_o} - \frac{P_o}{2}}{1 - \zeta} \qquad (K > 0) \qquad (22)$$

$$\omega_o = \frac{\sqrt{Q_o} + \frac{P_o}{2}}{1 + \zeta} \qquad (K < 0) \qquad (23)$$

for the values at the cusp points. These values are given by the two curves in figure 10. The maximum damping for negative K at any value of ζ may then be obtained by using equation (23) in equation (14) to yield

$$R_{max} = -\frac{P_o}{4} - \left(\frac{\sqrt{Q_o}}{2} + \frac{P_o}{4}\right)\frac{\zeta}{1 + \zeta} \qquad (K < 0) \qquad (24)$$

If the values of P_o and Q_o for the Dutch roll of the airplane under consideration are used and ζ is taken equal to 0.3, equation (24) shows that the maximum damping with negative gearing corresponds to $T_{1/2} = 1.0$ second.

Figure 15 shows the curve for this value of damping. The cusp point for negative gearing occurs at $\omega_o = 3.96$ radians per second and $K = -0.035$ deg/deg/sec. For positive gearing, on the other hand, an infinite range of ω_o values which will give better than this damping with $\zeta = 0.3$ is seen to be available. This bears out the previous statement that the design, with regard to damping ratio and natural frequency, of a compromise autopilot which will improve a variety of flight conditions is less restricted when positive gearing is used.

Since the curve of figure 15 is typical of the curves for dampings somewhat greater than the airplane damping, it will be discussed in more detail. The curve has two separate branches and the discontinuity occurs between $\omega = 4.8$ radians per second and $\omega = 5$ radians per second. This critical frequency actually is $\omega_{cr} = \sqrt{Q_o - R^2}$ (see eq. (21a)). From what has been said previously, the portion of the curve of greatest interest is the second half (for positive K). This starts at the critical frequency at $\omega_o = \infty$ and $K = -\frac{P_o + 2R}{C_1}$. This value of K is the value for which an ideal autopilot (one with no lags) would yield the given damping, and will be denoted as K_o. The bottom part of the boundary can be seen to represent the values of K and ω_o which make the

airplane mode have the given damping, since the critical frequency is near the airplane frequency. On the other hand, the top part of the boundary represents the values of K and ω_o at which the autopilot mode has the given damping, since the values of ω along this part of the curve are very close to the corresponding values of ω_o.

Figure 16 shows the boundary for $T_{1/2} = 0.60$ second. The loops for negative damping have disappeared. This curve is the cusp curve for positive K, obtained by using equation (22) in equation (14). This fact has little practical significance, however, since there is no fundamental change in the shape of the curves at this damping.

For large values of damping, further changes occur in the type of damping curves in the $K\omega_o$-plane. For small values of R, equation (21a) gives real solutions for ω_o with any value of ω. However, for larger values of R the discriminant of equation (21a) changes sign for certain combinations of ω and R, so that no real solutions for ω_o exist. Setting this discriminant equal to zero yields

$$(\omega^2 + R^2)^2 + \left[\zeta^2(P_o + 2R)^2 - 2R(P_o + 2R) - 2Q_o\right](\omega^2 + R^2) + Q_o\left[Q_o + 2R(P_o + 2R)\right] = 0 \tag{25}$$

When this equation has a positive, real root for the quantity $\omega^2 + R^2$, this root determines the range of real values of ω for which the solutions for ω_o in equation (21a) are complex. The value of R for which real roots occur in equation (25) is obtained by equating the discriminant of this equation to zero to give

$$\left(1 - \zeta^2\right)R^2 - \left(1 - \zeta^2\right)\zeta^2 P_o R + \zeta^2\left(\frac{1}{4}P_o^2\zeta^2 - Q_o\right) = 0 \tag{26}$$

For the airplane being considered, with $\zeta = 0.3$, the values of R obtained from equation (26) are $R = -1.58$ and $R = 1.61$. Since only the positive-damping boundaries are of interest, only the negative value (which corresponds to $T_{1/2} = 0.44$ second) need be considered. For this value of damping, the range of values given by equation (25) becomes a single value. For greater damping, equation (25) gives a finite range of values of ω which will not occur at any real value of ω_o. Thus, no value of ω in this range can occur for the required damping when $\zeta = 0.3$. The constant-damping boundaries for these larger values of damping, which are characterized by the absence of a given range of ω values, are of a somewhat different type from the curves for lower damping.

As an example of the type of curve which occurs for large damping values, the boundary for $T_{1/2} = 0.25$ second $(R = -2.77)$ is presented in figure 17. Substituting $\zeta = 0.3$ and $R = -2.77$ into equation (25) gives $\omega = 4.3$ radians per second and $\omega = 6.3$ radians per second. That is, no values of ω in the range $4.3 < \omega < 6.3$ radians per second occur on this curve. Some of the significant features of this curve will now be described, since it is typical of the higher-damping curves.

The significant portion of this curve defines the same general type of wedge-shaped good region as was present for lower dampings. On the lower part of the significant boundary, the frequency of the mode with the given damping is in the range $4.0 < \omega < 4.3$ radians per second; that is, the frequency varies between the critical frequency and the smaller frequency given by equation (25). These frequencies clearly represent the airplane mode. At the point of the wedge the previously discussed discontinuity appears. At this point both the airplane and autopilot modes have the same damping. On the upper part of the boundary the autopilot mode has the required damping and the airplane mode has higher damping.

Figure 18 is a collection of the significant portions of the damping curves previously discussed. This figure shows that, as the required damping increases, the wedge-shaped region in the positive $K\omega_o$-plane which insures this amount of damping moves upward and to the right. The figure also shows that the damping obtainable with a second-order yaw autopilot cannot always be increased merely by increasing the gearing ratio. The reason is that, for a given value of ω_o, increasing K beyond a certain value makes the autopilot mode less stable. Clearly, more damping can be obtained by increasing ω_o at the same time that K is increased. These results confirm the statement made in the discussion of figure 10 that it may be necessary to increase the natural frequency when the gain is increased.

It is important to remember that, as in the $\zeta\omega_o$-plane, two oscillations are present in the regions of most interest in the $K\omega_o$-plane. The typical frequencies given on the individual boundaries indicate that the portions of the wedge-shaped boundaries where K is high correspond to the autopilot mode having the given damping, whereas the parts where K is low correspond to the airplane mode having the given damping.

Figure 18 seems to indicate that an infinite amount of damping might be obtainable by simultaneously increasing K and ω_o, in contradiction to the discussion concerning figures 10 and 11. However, further changes occur in the type of curve at larger dampings. Equation (21a) indicates that a change might be expected when $R > \sqrt{Q_o}$, since the quantity $Q_o - R^2 - \omega^2$ does not go through zero for any value of ω. That

is, there no longer is a critical frequency $\omega_{cr} = \sqrt{Q_o - R^2}$. Moreover, the good regions as previously shown do not take into account the boundary of equal roots. That is, within the good regions no oscillation has less damping than the indicated amount; however, a real root with less damping than the indicated amount may be present at points above the boundary of equal roots. The explanation is as follows. At the $\omega = 0$ point of a given high-damping curve (which point is on the boundary of equal roots) there are two equal real roots with the indicated amount of damping. However, at points above the boundary of equal roots, one of these real modes will decrease in damping. The oscillatory mode which breaks down into two real modes at the boundary of equal roots in the $K\omega_o$-plane is the airplane mode, since, as can be seen from figure 18, oscillations at autopilot frequency do occur above the boundary of equal roots. Thus, for points above this boundary the airplane mode becomes nonoscillatory. The physical reason for this phenomenon is that large gearing ratios cause the airplane mode to be overdamped. The boundary of equal roots in the $\zeta\omega_o$-plane, on the other hand, corresponds to large ζ values. Therefore, as can be seen from the curves, the mode which is overdamped at points above this boundary is the autopilot mode.

Strictly speaking, the boundary of equal roots should be considered as the upper limit of the good regions shown in figure 18. Actually, this restriction is necessary only for the regions of very high damping. For example, when the point $K = 0.60$ deg/deg/sec and $\omega_o = 21.5$ radians per second is taken on the boundary for $T_{1/2} = 0.60$ second in figure 18 and the characteristic roots are found, the autopilot mode has the given damping $T_{1/2} = 0.60$ second at $\omega = 21$ radians per second, whereas the airplane oscillation breaks down into two well-damped nonoscillatory modes with $T_{1/2} = 0.22$ second and $T_{1/2} = 0.09$ second. Thus, for this moderate damping, points above the boundary of equal roots still give the required damping.

For extremely large values of damping, however, the boundary of equal roots becomes important. In fact, the maximum damping of the complete system at a fixed value of ζ is the largest negative value of R occurring on the boundary of equal roots. The points on the boundary of equal roots are obtained by using $\omega = 0$ in equations (21a) and (21b). The largest value of R occurring on the boundary is obtained by setting the discriminant of equation (21a) equal to zero with $\omega = 0$. This procedure gives the quartic in R (from eq. (25) with $\omega = 0$):

$$\left(4\zeta^2 - 3\right)R^4 + 2P_o\left(2\zeta^2 - 1\right)R^3 + \left(\zeta^2 P_o^2 + 2Q_o\right)R^2 + 2P_oQ_oR + Q_o^2 = 0 \quad (27)$$

The largest negative real root of this equation is the value of the maximum damping. For the example considered, this value is $R = -5.11$ and the corresponding $T_{1/2} = 0.14$ second. For this value of damping, the good region becomes a single point on the boundary of equal roots. The airplane mode is a double real root equal to -5.11, and the autopilot mode is an oscillation with the same amount of damping. The autopilot characteristics for this maximum-damping point were used in calculating the motion subsequent to a 5° sideslip disturbance (fig. 19). For practical purposes, the airplane motion can be considered as nonoscillatory, since the autopilot oscillator is of too high a frequency to have an appreciable effect on the airplane. The well-damped nature of the Dutch roll motion (which has now become nonoscillatory) is evident in the β-motion. The slow return of the roll motion is due to the spiral mode. Although the lightly damped spiral mode is generally not considered troublesome, it is necessary to keep in mind that the discussion in this paper deals only with the improvement of the damping of the Dutch roll mode, and that the two aperiodic modes in the airplane's lateral motion have been ignored.

Effect of varying ζ on curves in the $K\omega_o$-plane.- In order to obtain an idea of the effect of changing ζ on the curves in the $K\omega_o$-plane, a comparison of the boundary of equal roots, the airplane damping boundary, and the boundary for $T_{1/2} = 0.60$ second is presented in figure 20 for $\zeta = 0.3$, 0.6, and 0.9. Although the region of improved damping with negative gearing increases in size, the narrowness of the frequency range and the other difficulties previously mentioned still make the use of negative gearing impractical. The increased slope of the upper part of the boundaries simply implies, as would be expected, that for larger values of ζ, larger values of K are required at any value of ω_o to make the autopilot mode become unstable. The variation in the position of the boundary of equal roots simply implies that the more highly damped mode associated with each point on a given boundary tends to become critically damped at lower gearings as ζ increases.

None of these variations appear to be very important practically. Indeed, the most important fact about the effect of varying ζ is that the bottom part of the boundary approaches the same value of K at large values of ω_o for all values of ζ. This behavior is due to the fact that the asymptotic value of K is K_o, the value required to obtain the given amount of damping with an ideal autopilot. Now, the bottom part of the boundary can be seen to be the important part, since it gives the lowest value of K for which the system has the required damping; also, the mode which attains the required damping at the points on this part of the boundary is the airplane mode. The flatness and invariance with ζ of the bottom part of the boundary imply that the minimum value of K for which a given damping may be attained is relatively invariant for changes in ζ and ω_o at fairly large values

of ω_o. This fact will be used in the next section to obtain a simple rule-of-thumb method for designing an efficient yaw-rate damper which will insure a required damping for several extreme flight conditions of an airplane using low gearing.

Design of Compromise Yaw-Rate Damper

For the sake of simplicity, the autopilot to be designed will be assumed to provide only a yawing moment proportional to yawing velocity, as in the previous analysis. It may therefore be called a C_{n_r} autopilot. Values of K, ζ, and ω_o which will efficiently improve the damping of an airplane in various flight conditions are desired. The criterion of the efficiency of the autopilot will be that the gearing ratio required for the autopilot must be small. This means that the autopilot power required will be small. Moreover, the use of small gearing makes the yaw damper easier to override in steady turns.

Table II gives the parameters used for the three flight conditions of the airplane chosen for the present example. Case I is a high-lift-coefficient, low-wing-loading landing condition at sea level. Case II is a low-lift-coefficient, medium-wing-loading cruising condition at 30,000 feet. To complete the picture, case III is a high-lift-coefficient, high-wing-loading cruising condition at 30,000 feet. These cases will serve as examples to illustrate the method.

Table II shows that the Dutch roll oscillation in case II is very poorly damped, since it requires almost 7 seconds to damp to one-half amplitude. Although the other two cases are not so poorly damped, they are still unsatisfactory. Calculated motions for the three cases in response to a 5° disturbance in sideslip are shown in figure 21. No attempt will be made to set up any complicated criteria for adequate damping. Instead, the criterion chosen for purposes of illustration will be that the Dutch roll oscillation should damp to one-half amplitude in 1 second or less at any flight condition. Actually, the autopilot may be designed to insure a different amount of damping for each flight condition, in case one of the flight conditions is required to be more stable than another.

The fundamental problem is to find the set of points (K,ω_o,ζ) which satisfy the given damping criterion for all three flight conditions. Moreover, the minimum possible gearing is desired. The value of K_o for $T_{1/2} = 1$ second is calculated for each flight condition. From the equivalent-oscillator analysis, the value of K_o is shown to be

$$K_o = \frac{1}{C_1}\frac{1.386}{T_{1/2}} - P_o$$

Substitution from table II gives the values of K_o as 0.1213, 0.0698, and 0.1374 deg/deg/sec for cases I, II, and III, respectively.

If the largest of these values of K_o (corresponding to case III) is chosen for the gearing of the autopilot, the curve for $T_{1/2} = 1$ second in the $\zeta\omega_o$-plane will be the critical curve for case III, but for cases I and II the curve for $T_{1/2} = 1$ second will be a curve between the airplane damping and the critical damping. Each of these three curves defines an infinite region in the upper right portion of the $\zeta\omega_o$-plane as the region insuring better damping. Therefore, in the $\zeta\omega_o$-plane an infinite region of points which are common to these three regions must exist and can be used with this value of K to obtain better damping than $T_{1/2} = 1$ second for all three flight conditions. A plot of these regions is shown in figure 22(a), where $K = 0.14$ deg/deg/sec has been used. The plot shows that any set of values in the $\zeta\omega_o$-plane which insures $T_{1/2} = 1$ second for case II, the high-frequency case, will also insure this amount of damping for the other two cases. However, any point in this region is at a value of ω_o considerably above the optimum for cases I and III. As was previously pointed out, for such values of ω_o the minimum value of K for which a given damping may be obtained does not differ much from K_o. The implication is that the minimum value of K for which $T_{1/2} = 1$ second may be insured for case III, while at the same time $T_{1/2}$ remains less than 1 second for case II, is not much less than 0.1374 deg/deg/sec. To confirm this hypothesis, the necessary points on the curves in the $\zeta\omega_o$-plane for $T_{1/2} = 1$ second were obtained for $K = 0.12$ deg/deg/sec and $K = 0.10$ deg/deg/sec, and the significant parts of these curves are shown in figures 22(b) and 22(c).

For values of $K < 0.1374$ deg/deg/sec the curve for $T_{1/2} = 1$ second for case III must be a loop, since the damping is higher than the critical damping. Figure 22(b) shows that when $K = 0.12$ deg/deg/sec this loop is still large enough to intersect the region where $T_{1/2} < 1$ second for case II. The hatched region on figure 22(b) is the region which will insure $T_{1/2} < 1$ second for all three flight conditions at $K = 0.12$ deg/deg/sec. Figure 22(c) shows that the loop for case III has become too small to intersect the region where $T_{1/2} < 1$ second for case II when $K = 0.10$ deg/deg/sec. Therefore, a value of $T_{1/2} < 1$ second

cannot be obtained for cases II and III simultaneously when $K = 0.10$ deg/deg/sec. The curve for case I is not shown in this figure since, as seen in figures 22(a) and 22(b), it is not necessary.

The discussion of figure 22 shows that, in order to improve all the flight conditions in the present example with a single second-order autopilot, a gearing ratio has to be used which is almost as large as would be needed for an ideal autopilot that would stabilize all the flight conditions. This difficulty arises because the low-frequency conditions require the highest values of K_o, as can be seen by examining the approximate expression for the frequency of the Dutch roll oscillation at any flight condition and the associated expression for K_o:

$$\omega_A^2 \approx \frac{V^2}{b^2} \frac{C_{n_\beta}}{2\mu_b\left(K_Z^2 - \frac{K_{XZ}^2}{K_X^2}\right)} \tag{28a}$$

$$K_o = -\frac{b^2}{V^2} \frac{2\mu_b\left(K_Z^2 - \frac{K_{XZ}^2}{K_X^2}\right)(P - P_o)}{C_{n_\delta}} \approx \frac{-C_{n_\beta}}{C_{n_\delta}} \frac{(P - P_o)}{\omega_A^2} \tag{28b}$$

Because of the possibility of variations in C_{n_β}, C_{n_δ}, and $P - P_o$ in the various flight conditions, it is not possible to state that in general the low-frequency flight conditions will require the higher values of K_o, as is true in the present example. When the highest required value of K_o occurs at the high-frequency conditions, the minimum value of K for the compromise autopilot may be considerably below this highest required value, because the region of overlap similar to that shown in figure 22(b) will include the optimum point for the high-frequency condition.

In any case, the characteristics of the compromise autopilot can be obtained by plotting the regions insuring the required damping for the various conditions at various values of K below the maximum value of K_o, as is done in figure 22. The value of K which leads to a small overlap region is then the minimum compromise gearing, and the values in the overlap region of the $\zeta\omega_o$-plane define the possible values for ζ and ω_o of the compromise autopilot.

A convenient method is available for determining the range of values of K to be used in obtaining the overlap region. The values of K_o and the optimum value of K which will yield the required damping for each of the flight conditions are calculated. Then the compromise value of K must lie between the highest optimum value of K and the highest value of K_o. In making the plots it may soon become clear that some of the flight conditions do not need to be considered, as happened with case I in the present example.

In the present example, it has been shown that a gain much smaller than the largest value of K_o necessary cannot be used, unless a variable gain is available. If a constant gain must be used at all flight conditions of such an airplane, a simple rule of thumb for designing the autopilot would be to choose the largest value of K_o (corresponding to the low-frequency conditions) and values of ζ and ω_o near the optimum point of the high-frequency condition. In this way some advantage is derived from the second-order characteristics of the autopilot in that the damping obtained from the autopilot is much larger for the high-frequency conditions than that which would result from an ideal autopilot with this gearing.

In applying this simple method, 0.14 deg/deg/sec was chosen for the value of K, and the optimum point was found for case II. The optimum point was $\zeta = 0.523$ and $\omega_o = 9.49$ radians per second. Figure 23 shows the calculated motions for the three flight conditions with this autopilot, subsequent to a 5° sideslip disturbance. A comparison of figure 23 with figure 21 reveals that the stability of all three flight conditions is improved. In particular, case II is greatly improved, while cases I and III both have $T_{1/2}$ slightly less than 1 second.

Since the results of figure 21(b) show that a gearing of 0.12 deg/deg/sec could have been used, the optimum point for case II was calculated for this gearing and found to be $\zeta = 0.485$ and $\omega_o = 8.81$ radians per second. Figure 24 shows the motions in the three flight conditions with these autopilot characteristics. A comparison of this figure with figure 23 reveals that the damping obtained with this autopilot is only slightly less than the damping obtained when K = 0.14 deg/deg/sec.

If the low-frequency conditions require little improvement, the problem approaches that of improving only a single flight condition, so that the optimum-point characteristics may be used to decrease the gearing necessary. For example, suppose that $T_{1/2} = 1.5$ seconds had been considered satisfactory for the low-frequency conditions. The value of K_o necessary to obtain this damping is 0.075 deg/deg/sec,

and the corresponding optimum point for case II is $\zeta = 0.389$ and $\omega_o = 7.40$ radians per second. The improvement of the stability of the various flight conditions may be seen from the motions presented in figure 25. In these motions the value of $T_{1/2}$ for cases I and III is between 1 and 1.5 seconds, but the value of $T_{1/2}$ for case II is well under 1 second.

It is clear from the previous discussion that for the present example an autopilot with fixed characteristics would require a large gain (corresponding to the largest value of K_o) in order to improve both landing and cruising flight conditions. A variable gain would therefore be desirable, so that this excessive gearing would not have to be used at the higher speeds. Although it would be impractical to expect that all three autopilot parameters should be variable in flight, as would be desirable to obtain the optimum autopilot for each flight condition, it would be relatively simple to make the gain variable. The value of ζ chosen would be that of the optimum point for the high-frequency condition (as calculated for the low-gearing value), and the value of ω_o would be preferably slightly above the optimum value of ω_o for the high-frequency condition. (Because of the rapid change in damping at values of ω_o less than the optimum, in practice a safety factor should generally be added to this value.) In such cases, probably only two gain positions would be necessary - a high gain for the low-velocity conditions and a low gain for the high-velocity conditions. Thus, low gain could be used in the high-velocity flight conditions, so that the adverse effects of the autopilot in steady turns at high velocity would be small.

Validity of Assuming Pure C_{n_r} Autopilot

A few final remarks will be made concerning the assumption that the autopilot is sensitive to yawing velocities only, and provides yawing moments only. For practical autopilot installations, the sensing device (usually a gyroscope) is fixed in the airplane. The device is therefore sensitive to yawing velocities about some axis fixed in the airplane. The equations of motion, however, are set up with respect to the stability axes. For various flight conditions, the angle of inclination between the gyro axes and the stability axes varies because of the varying angle of attack. This angle of inclination makes the gyroscope sensitive also to rolling velocity about the stability axes. In addition, the displacement of the autopilot-actuated control surface from the longitudinal stability axis gives rise to rolling moments. As shown in reference 10, these two effects cause increments in C_{n_p}, C_{l_r}, and C_{l_p} due to the autopilot, in addition to the expected C_{n_r} increment. The C_{n_p} effect is the most important of these in affecting the Dutch roll stability of the airplane, and this effect will now be discussed.

When the stability of a single flight condition is to be improved, the C_{n_p} effect may be removed by orienting the gyro axis along the flight path, and no modification of the results is necessary. If an angle of gyro inclination does exist, the general method of setting up the constant-damping boundaries is, of course, still valid. In order to take account of the C_{n_p} effect, $D\psi$ is simply replaced in equation (6) by the proper linear combination of $D\psi$ and $D\phi$, as shown in reference 10. Because of the presence of the $D\phi$ term all three degrees of freedom must be used, and the equivalent-oscillator simplification can no longer be used. Thus, the method is more complicated when the C_{n_p} effect of the autopilot is not small enough to be neglected. When the C_{n_p} effect becomes excessively large, the problem becomes even more complicated because of the fact that the damping of the aperiodic modes becomes important, and curves of constant damping for these modes (corresponding to real roots) have to be plotted. In fact, the aperiodic modes may combine to form another oscillation.

In considering the problem of simultaneously stabilizing various flight conditions which have various angles of attack, the C_{n_p} effect must always be considered unless the gyro axis can somehow be rotated so that it is always parallel to the relative-wind axis. The C_{n_p} effect can sometimes be ignored, if the angle-of-attack range of the flight conditions is small, by choosing an orientiation of the gyroscope in such a direction that all the angles of inclination are small. Because of the extreme complexity of the problem when the C_{n_p} effects must be considered, this paper is confined to the consideration of C_{n_r} effects only.

CONCLUDING REMARKS

The damping of an oscillatory system that makes use of a second-order rate damper with a given gearing ratio K can be improved by adjusting the shape of the autopilot frequency response (that is, the damping ratio and the natural frequency of the autopilot). For the purpose of determining the effect of a second-order yaw-rate damper on the damping of the Dutch roll motion of an airplane in a given flight condition, the airplane may be represented as an equivalent oscillator. By using this equivalent-oscillator concept, the optimum shape of the autopilot frequency response corresponding to a given gearing ratio or required damping may be obtained from a simple set of equations for any flight condition. The gearing ratio necessary to obtain a given amount of damping when the damping ratio and natural frequency of the autopilot are near their optimum values is considerably less than the gearing ratio necessary to obtain the same amount of damping with an idealized (no-lag) autopilot.

The problem of designing a second-order yaw damper for an airplane which requires improvement in damping for several flight conditions is more complicated, since for each flight condition the airplane is represented by a different equivalent oscillator. However, a simple method of compromise is derived for flight conditions in which the effect of the yaw-damper sensitivity to rate of roll is small enough to be neglected.

The effects of a second-order yaw damper on the stability of any given flight condition of an airplane can be obtained by examining the constant-damping curves in the plane of the damping ratio and natural frequency of the autopilot and in the plane of the gearing ratio and natural frequency of the autopilot. Theoretically, any given flight condition may be stabilized by using either positive or negative gearing. When negative gearing is used, the autopilot natural frequency must be less than the airplane frequency. The use of negative gearing is shown to be impractical, however. For positive gearing, the autopilot natural frequency must be greater than the airplane frequency.

For fixed positive gearing, there is an infinite number of combinations of autopilot natural frequency and damping ratio for which the second-order autopilot gives better damping than an ideal autopilot of the same gearing. For fixed positive damping ratio of the autopilot, there is a range of values of positive gearing ratio which will provide a given damping to the system at any autopilot natural frequency greater than the airplane frequency. Increasing the gearing ratio of the autopilot to excessive values will always cause the autopilot mode of oscillation to become unstable for a given damping ratio and natural frequency of the autopilot. If larger gearing ratios are to be used in order to obtain higher stability for the airplane mode, the damping ratio or the natural frequency of the autopilot, or both, must be increased. Expressions are derived for the maximum damping under various conditions.

Langley Aeronautical Laboratory,
National Advisory Committee for Aeronautics,
Langley Field, Va., October 2, 1952.

APPENDIX A

EXPRESSIONS FOR CONSTANT-DAMPING CURVES AND DISCUSSION OF EQUIVALENT-OSCILLATOR CONCEPT

Since the characteristic equation of the airplane-damper system is of sixth degree, as given in equation (7), it may be written

$$F(D) = D^6 + A_5D^5 + A_4D^4 + A_3D^3 + A_2D^2 + A_1D + A_0 = 0 \qquad (A1)$$

Here A_5, A_4, . . . A_0 are functions of K, ζ, and ω_o for a flight condition in which the airplane parameters in equations (3) to (5) are known. If any one of the three autopilot parameters is fixed, stability boundaries may be obtained in the plane defined by the other two parameters by letting $D = R + i\omega$, fixing the value of R for each curve, and varying ω. Since equation (A1) is a complex equation, it may be written as two real equations and solved for the two autopilot variable parameters at each value of $D = R + i\omega$.

According to reference 6, if

$$f_n(R) = \frac{1}{n!}\frac{d^nF(R)}{dR^n} \qquad (n = 1,2,3,\ldots) \qquad (A2)$$

then the two real equations obtained from equation (A1) by setting D equal to $R + i\omega$ are

$$F(R) - \omega^2 f_2(R) + \omega^4 f_4(R) - \omega^6 = 0 \qquad (A3)$$

$$f_1(R) - \omega^2 f_3(R) + \omega^4 f_5(R) = 0 \qquad (A4)$$

Since the coefficients of $F(R)$ and $f_n(R)$ are functions of the two variable autopilot parameters only, the values of these two parameters which will yield an oscillatory mode of motion with a given damping may be obtained by choosing a value for R and solving equations (A3) and (A4) at any value of ω. This procedure yields a point

on the given R curve in the parameter plane; for instance, in the $\zeta\omega_o$-plane if ζ and ω_o be chosen as the variable parameters. In this case, calculations are simplified by the use in equations (A3) and (A4) of A and B as defined in equation (1), since these equations become linear in A and B.

Because of the increasing difficulty of obtaining accurate values of stability derivatives for present-day airplanes, the characteristics of the airplane may be given in terms of transfer functions which are obtained from flight data. In order to obtain the form of the characteristic equation in terms of transfer functions, equation (7) is divided through by $\left(D^2 + 2\zeta\omega_o D + \omega_o^2\right)F_o(D)$. The resulting equation is

$$1 - \frac{K\omega_o^2}{D^2 + 2\zeta\omega_o D + \omega_o^2}\left[\frac{V^2}{b^2} C_{n_\delta} \frac{\left(2\mu_b D - \frac{V}{b} C_{Y_\beta}\right)\left(2\mu_b K_X^2 D^2 - \frac{V}{2b} C_{l_p} D\right) + \frac{V^3}{b^3} C_L C_{l_\beta}}{F_o(D)}\right] = 0$$

The first factor in the second term of this equation is the autopilot transfer function $\left[\frac{\delta}{D\psi}\right]_P(D)$ (See eq. 8.) If equations (3) to (5) are solved operationally for zero initial conditions, the expression in brackets is found to be the airplane transfer function:

$$\left[\frac{D\psi}{\delta}\right]_A(D) = \frac{V^2}{b^2} C_{n_\delta} \frac{\left(2\mu_b D - \frac{V}{b} C_{Y_\beta}\right)\left(2\mu_b K_X^2 D^2 - \frac{V}{2b} C_{l_p} D\right) + \frac{V^3}{b^3} C_L C_{l_\beta}}{F_o(D)} \qquad (A5)$$

Therefore, the characteristic equation may be written

$$1 - \left[\frac{\delta}{D\psi}\right]_P(D)\left[\frac{D\psi}{\delta}\right]_A(D) = 0 \qquad (A6)$$

in terms of the autopilot and airplane transfer functions. The airplane transfer function for the lateral motion, as shown in equation (A5), should have the form of a cubic in D over a quartic in D. Therefore, when equation (A6) is cleared of fractions a sixth-degree equation of the form of equation (A1) is again obtained as the characteristic equation.

The setup and solution of equations (A3) and (A4) would be greatly simplified if the characteristics of the airplane lateral motion could be expressed as a second-order system rather than a fourth-order system. Since the yaw damper is used essentially for damping the Dutch roll oscillation, it was thought desirable to see whether the airplane could be replaced by an equivalent oscillator whose damping and period were those of the Dutch roll oscillation of the airplane. That is, if the Dutch roll mode, as calculated when three degrees of freedom are considered, is obtained from the quadratic equation $D^2 + P_oD + Q_o = 0$, the question is whether the airplane characteristics may be represented by the oscillator described by

$$2\mu_b\left(K_Z{}^2 - \frac{K_{XZ}{}^2}{K_X{}^2}\right)\left(D^2 + P_oD + Q_o\right) = 0$$

Equation (A5) may be rewritten in the form

$$\left[\frac{D\psi}{\delta}\right]_A(D) = \left[\frac{\frac{V^2}{b^2}Cn_\delta D}{2\mu_b\left(K_Z{}^2 - \frac{K_{XZ}{}^2}{K_X{}^2}\right)\left(D^2 + P_oD + Q_o\right)}\right]\left[\frac{(D + a_1)\left(D^2 + a_2D + a_3\right)}{D\left(D^2 + a_4D + a_5\right)}\right]$$

$$= \left[\frac{-C_1D}{D^2 + P_oD + Q_o}\right]\left[\frac{(D + a_1)\left(D^2 + a_2D + a_3\right)}{D\left(D^2 + a_4D + a_5\right)}\right] \qquad (A7)$$

where the constant C_1 is defined by

$$C_1 = -\frac{V^2Cn_\delta}{2b^2\mu_b\left(K_Z{}^2 - \frac{K_{XZ}{}^2}{K_X{}^2}\right)}$$

The expression in the first bracket on the right-hand side of equation (A7) is the same as would be obtained for $\left[\frac{D\psi}{\delta}\right]_A(D)$ if the assumption were made that the airplane could be represented by the equivalent oscillator described previously. Thus, if the expression in the second bracket has a frequency response which does not significantly differ

from unity for the range of frequencies which is important in the airplane frequency response, then the expression in the first bracket can be used as a valid approximation to the airplane frequency response. Therefore, the expression in the second bracket can be considered as a correction function.

The factor $D^2 + a_4D + a_5$ yields the two real characteristic roots of the airplane lateral motion corresponding to the spiral mode and the damping-in-roll mode. The usual approximation to the damping-in-roll root is $VC_{l_p}/4b\mu_b K_X^2$, and the spiral root is of the order of $VC_{Y_\beta}/2b\mu_b$. However, the numerator of the second bracket can be shown to be

$$D^3 - \frac{V}{b}\left(\frac{C_{Y_\beta}}{2\mu_b} + \frac{C_{l_p}}{4\mu_b K_X^2}\right)D^2 + \frac{V^2}{b^2}\frac{C_{l_p}C_{Y_\beta}}{8\mu_b K_X^2}D - \frac{V^3}{b^3}\frac{C_L C_{l_\beta}}{4\mu_b{}^2 K_X^2}$$

If $C_{l_\beta} = 0$, this cubic has the roots

$$D = 0 \qquad D = \frac{C_{Y_\beta}}{2\mu_b}\frac{V}{b} \qquad D = \frac{C_{l_p}}{4\mu_b K_X^2}\frac{V}{b}$$

which are merely approximations to the real roots which occur in the cubic in the denominator of equation (A7). It can therefore be expected that the second bracket will usually be close to unity and that no large errors will arise if the airplane lateral motion is represented by a single-degree-of-freedom oscillator in yaw with nondimensional inertia $2\mu_b\left(K_Z^2 - \frac{K_{XZ}^2}{K_X^2}\right)$ and the same period and damping as the Dutch roll oscillation. This is especially true for small values of C_{l_β}.

For the airplane used as an example in this paper, the correction function $\frac{(D + a_1)(D^2 + a_2D + a_3)}{D(D^2 + a_4D + a_5)}$ was evaluated throughout the frequency range and its effect on the total airplane transfer function was found to be very small except close to zero frequency. Finally, actual comparisons of the stability boundaries for the three-degree-of-freedom analysis and the equivalent-oscillator approximation showed that the approximation was valid.

When equation (A7) is used with this approximation, the characteristic equation as given in equation (A6) becomes

$$1 + \left[\frac{K\omega_o^2}{D^2 + 2\zeta\omega_o D + \omega_o^2}\right]\left[\frac{C_1 D}{D^2 + P_o D + Q_o}\right] = 0$$

or

$$2\mu_b\left(K_Z^2 - \frac{K_{XZ}^2}{K_X^2}\right)\left(D^2 + P_o D + Q_o\right)\left(D^2 + 2\zeta\omega_o D + \omega_o^2\right) - \frac{V^2}{b^2} K\omega_o^2 C_{n_\delta} D = 0 \tag{A8}$$

The characteristic equation of the system is therefore a quartic,

$$\begin{aligned} F(D) &= D^4 + \left(P_o + 2\zeta\omega_o\right)D^3 + \left(Q_o + \omega_o^2 + 2\zeta\omega_o P_o\right)D^2 + \\ &\quad \left(P_o\omega_o^2 + 2\zeta\omega_o Q_o + C_1 K\omega_o^2\right)D + Q_o\omega_o^2 \\ &\equiv D^4 + \left(P_o + A\right)D^3 + \left(Q_o + B + AP_o\right)D^2 + \\ &\quad \left(P_o B + Q_o A + C_1 KB\right)D + Q_o B \\ &= 0 \end{aligned} \tag{A9}$$

The equations for the stability boundaries which replace equation (A3) and equation (A4) for a fourth-order characteristic equation are

$$F(R) - \omega^2 f_2(R) + \omega^4 = 0 \tag{A10}$$

$$f_1(R) - \omega^2 f_3(R) = 0 \tag{A11}$$

The functions $f_n(R)$ are obtained from equation (A2).

As an example, the actual parametric equations used for the equivalent oscillator will be derived. Equation (A9) is used in equation (A2) to give

$$f_1(R) = 4R^3 + 3R^2(P_o + A) + 2R(Q_o + B + AP_o) + (P_o + C_1K)B + Q_oA$$

$$f_2(R) = 6R^2 + 3R(P_o + A) + Q_o + P_oA + B$$

$$f_3(R) = 4R + P_o + A$$

These expressions are used in equations (A10) and (A11). To obtain the constant-K curves (that is, curves in the AB-plane or $\zeta\omega_o$-plane), the resulting equations are written in A and B, as follows:

$$\left[(3R + P_o)\omega^2 - R\left(R^2 + P_oR + Q_o\right)\right]A + \left\{\omega^2 - \left[R^2 + (P_o + C_1K)R + Q_o\right]\right\}B =$$

$$\omega^4 - \left(6R^2 + 3P_oR + Q_o\right)\omega^2 + R^2\left(R^2 + P_oR + Q_o\right) \tag{A12}$$

$$\left[\omega^2 - \left(3R^2 + 2P_oR + Q_o\right)\right]A - \left(2R + P_o + C_1K\right)B =$$

$$-(4R + P_o)\omega^2 + R\left(4R^2 + 3P_oR + 2Q_o\right) \tag{A13}$$

For a given value of K, any constant-damping curve is obtained by fixing R at the appropriate value and taking a sufficient number of positive values for ω to obtain the points necessary to determine the curve. The resulting two linear equations in A and B are solved to obtain each point. If curves in the $\zeta\omega_o$-plane are desired instead, the values of ζ and ω_o can be obtained for each set of values of A and B for which B is positive.

The constant-ζ curves in the $K\omega_o$-plane are obtained by solving the parametric equations for K and ω_o instead of for A and B. For example, solving equation (A13) for K gives

$$K = \frac{1}{C_1 B}\left\{(A + P_o + 4R)\omega^2 - \left[(P_o + 2R)B + \left(Q_o + 2P_oR + 3R^2\right)A + R\left(2Q_o + 3P_oR + 4R^2\right)\right]\right\}$$

$$= \frac{1}{C_1 \omega_o{}^2}\left\{(2\zeta\omega_o + P_o + 4R)\omega^2 - \left[(P_o + 2R)\omega_o{}^2 + 2\zeta\omega_o\left(Q_o + P_oR + 3R^2\right) + R\left(2Q_o + 3P_oR + 4R^2\right)\right]\right\} \tag{A14}$$

and using this equation in equation (A12) gives

$$\left(Q_o - R^2 - \omega^2\right)B - \left(P_o + 2R\right)\left(\omega^2 + R^2\right)A + \omega^4 - \left(Q_o + 2P_oR + 2R^2\right)\left(\omega^2 + R^2\right) =$$

$$\left(Q_o - R^2 - \omega^2\right)\omega_o{}^2 - 2\zeta\omega_o\left(P_o + 2R\right)\left(\omega^2 + R^2\right) + \omega^4 - \left(Q_o + 2P_oR + 2R^2\right)\left(\omega^2 + R^2\right) = 0 \tag{A15}$$

This equation is a quadratic in ω_o for fixed values of ζ, R, and ω. The values of ω_o from equation (A15) are then used in equation (A14) to obtain the points on the curves in the $K\omega_o$-plane. Since equations (A12) and (A13) are linear, there is only one point in the AB-plane or the $\zeta\omega_o$-plane for each oscillatory mode when K is fixed. However, for a fixed value of ζ there may be two points in the $K\omega_o$-plane for a given oscillatory mode when the quadratic equation (A15) has two real, positive roots for ω_o.

APPENDIX B

DERIVATION OF EXPRESSIONS FOR MAXIMUM-DAMPING CHARACTERISTICS WITH FIXED GEARING RATIO BY USE OF EQUIVALENT-OSCILLATOR CONCEPT

The characteristic equation of the airplane—yaw-damper system, for the assumption that the airplane may be replaced by an equivalent oscillator, is

$$D^4 + (P_o + A)D^3 + (Q_o + B + AP_o)D^2 + (P_oB + AQ_o + C_1KB)D + Q_oB = 0 \tag{B1a}$$

The conditions on A and B which result in the maximum damping for a given gearing ratio can be calculated as follows. For the case of maximum damping, equation (B1a) will have two pairs of equal complex roots; hence this equation becomes:

$$(D^2 + PD + Q)^2 = D^4 + 2PD^3 + (P^2 + 2Q)D^2 + 2PQD + Q^2 \tag{B1b}$$

where $D^2 + PD + Q$ is the quadratic corresponding to the double oscillatory root at the cusp point. The following four equations are obtained by equating like coefficients in equation (B1b):

$$2P = P_o + A \tag{B2}$$

$$P^2 + 2Q = Q_o + B + AP_o \tag{B3}$$

$$2PQ = P_oB + AQ_o + C_1KB \tag{B4}$$

$$Q^2 = Q_oB \tag{B5}$$

Since K, C_1, P_o, and Q_o are known, these four independent equations may be solved for A, B, P, and Q. Thus, the autopilot parameters which will give the highest damping to the Dutch roll oscillation, and also the period and damping of this oscillation, may be determined.

From equations (B2) and (B5)

$$A = 2P - P_o \tag{B6}$$

$$B = \frac{Q^2}{Q_o} \tag{B7}$$

Using equations (B6) and (B7) in equation (B4) yields

$$P = \frac{(P_o + C_1K)Q^2 - P_oQ_o^2}{2Q_o(Q - Q_o)} \tag{B8}$$

When equations (B6) and (B7) are used in equation (B3), the result may be written

$$Q_o(P - P_o)^2 = (Q - Q_o)^2 \tag{B9}$$

and by substituting equation (B8) into equation (B9) a quartic equation in Q is obtained, which may be written

$$\left[P_o(Q - Q_o)^2 + C_1KQ^2\right]^2 = 4Q_o(Q - Q_o)^4$$

Finally, this equation yields the two quadratics in Q:

$$\left(1 + \frac{C_1K}{P_o \pm 2\sqrt{Q_o}}\right)Q^2 - 2Q_oQ + Q_o^2 = 0 \tag{B10}$$

Evaluation of the discriminant of equation (B10) reveals that equation (B10) has only two real roots, one less than Q_o and the other greater than Q_o. As can be seen from figure 6, the smaller value of Q (which yields a smaller value of ω_o) corresponds to the breakdown of the unstable loops for positive K. The larger real root of equation (B10) is therefore the one which yields the maximum-damping point for positive gearing ratio. Negative gearing ratios will be discussed subsequently.

The corresponding value of P is obtained by substituting this larger root into equation (B8), and the maximum-damping point in the

AB-plane is easily obtained from equations (B6) and (B7). Thus, the value of the maximum damping of the Dutch roll oscillation obtainable with a given gearing ratio, and also the values of autopilot frequency and damping which will yield this maximum damping, may be obtained by simply solving a quadratic equation (eq. (B10)).

The procedure is even simpler when the required damping is given and the values for the autopilot parameters which would make this damping the maximum damping are to be determined. The value of P is determined by the required damping, since

$$P = -2R = \frac{1.386}{T_{1/2}} \tag{B11}$$

and the corresponding optimum value of A may be obtained from equation (B6). Equation (B9) now gives

$$Q = Q_o \pm \sqrt{Q_o}\,(P - P_o) \tag{B12}$$

Both values of Q obtained from equation (B12) correspond to optimum points, since they both correspond to the given positive value of damping. These values may now be used in equation (B7) to obtain the corresponding values of B. Finally, the two values of gearing ratio may be obtained from equation (B8), which gives

$$K = \frac{2PQ - P_oB - AQ_o}{C_1B} \tag{B13}$$

The smaller values of Q (obtained from using the minus sign in eq. (B12)) result in negative values of gearing ratio and values of ω_o less than the airplane frequency. The possibility of using negative gearing to improve the damping is discussed further in the body of the paper.

REFERENCES

1. Sternfield, Leonard: Effect of Automatic Stabilization on the Lateral Oscillatory Stability of a Hypothetical Airplane at Supersonic Speeds. NACA TN 1818, 1949.

2. Gates, Ordway B., Jr.: A Theoretical Analysis of the Effect of Several Auxiliary Damping Devices on the Lateral Stability and Controllability of a High-Speed Aircraft. NACA TN 2565, 1951.

3. Schade, Robert O., and Hassell, James L., Jr.: The Effects on Dynamic Lateral Stability and Control of Large Artificial Variations in the Rotary Stability Derivatives. NACA TN 2781, 1952.

4. Greenberg, Harry: Frequency-Response Method for Determination of Dynamic Stability Characteristics of Airplanes With Automatic Controls. NACA Rep. 882, 1947. (Supersedes NACA TN 1229.)

5. Ansoff, H. I.: Stability of Linear Oscillating Systems With Constant Time Lag. Jour. Appl. Mech., vol. 16, no. 2, June 1949, pp. 158-164.

6. Brown, W. S.: A Simple Method of Constructing Stability Diagrams. R. & M. No. 1905, British A.R.C., 1942.

7. Sternfield, Leonard, and Gates, Ordway B., Jr.: A Method of Calculating a Stability Boundary That Defines a Region of Satisfactory Period-Damping Relationship of the Oscillatory Mode of Motion. NACA TN 1859, 1949.

8. Sternfield, Leonard, and Gates, Ordway B., Jr.: A Theoretical Analysis of the Effect of Time Lag in an Automatic Stabilization System on the Lateral Oscillatory Stability of an Airplane. NACA Rep. 1018, 1952. (Supersedes NACA TN 2005.)

9. Gates, Ordway B., Jr., and Schy, Albert A.: A Theoretical Method of Determining the Control Gearing and Time Lag Necessary for a Specified Damping of an Aircraft Equipped With a Constant-Time-Lag Autopilot. NACA TN 2307, 1951.

10. Gates, Ordway B., Jr., and Sternfield, Leonard: Effect of an Autopilot Sensitive to Yawing Velocity on the Lateral Stability of a Typical High-Speed Airplane. NACA TN 2470, 1951.

TABLE I

PARAMETERS OF AIRPLANE USED AS EXAMPLE TO ILLUSTRATE USE OF CONSTANT-DAMPING CURVES

Altitude, ft	30,000
Wing loading, lb/sq ft	65
V, ft/sec	797
b, ft	28
C_L	0.23
μ_b	80.7
K_X^2	0.0097
K_Z^2	0.0513
K_{XZ}	-0.00145
C_{l_p}, per radian	-0.40
C_{l_r}, per radian	0.80
C_{n_p}, per radian	-0.02
C_{n_r}, per radian	-0.40
C_{Y_β}, per radian	-1.0
C_{n_β}, per radian	0.25
C_{l_β}, per radian	-0.126
C_{n_δ}, per radian	-0.163
Period, sec	1.3
$T_{1/2}$, sec	2.6
P_o, sec^{-1}	0.537
Q_o, sec^{-2}	23.84
C_1, sec^{-2}	15.98

TABLE II

PARAMETERS USED FOR THREE TYPICAL FLIGHT CONDITIONS OF THE AIRPLANE IN DESIGN OF COMPROMISE YAW-RATE DAMPER

	Case I	Case II	Case III
Altitude, ft	Sea level	30,000	30,000
Mach number	0.22	0.75	0.5
Wing loading, lb/sq ft	54	65	85
μ_b	25.2	81.25	106.3
K_X^2	0.0081	0.0069	0.0051
K_Z^2	0.0433	0.0419	0.0409
K_{XZ}	0.0027	0.0025	0.0010
C_L	0.765	0.262	0.771
C_{n_β}	0.205	0.205	0.212
C_{l_β}	-0.099	-0.107	-0.095
C_{Y_β}	-0.930	-0.878	-0.884
C_{l_p}	-0.425	-0.474	-0.435
C_{l_r}	0.288	0.200	0.300
C_{n_p}	0.003	0.010	0.003
C_{n_r}	-0.165	-0.150	-0.165
C_{n_δ}	-0.163	-0.163	-0.163
Period, sec	2.3	1.4	2.1
$T_{1/2}$, sec	2.0	6.9	2.4
P_o, sec^{-1}	0.704	0.200	0.573
Q_o, sec^{-2}	7.79	21.4	8.78
C_1, sec^{-2}	5.63	17.0	5.92
V/b, sec^{-1}	8.68	26.64	17.77

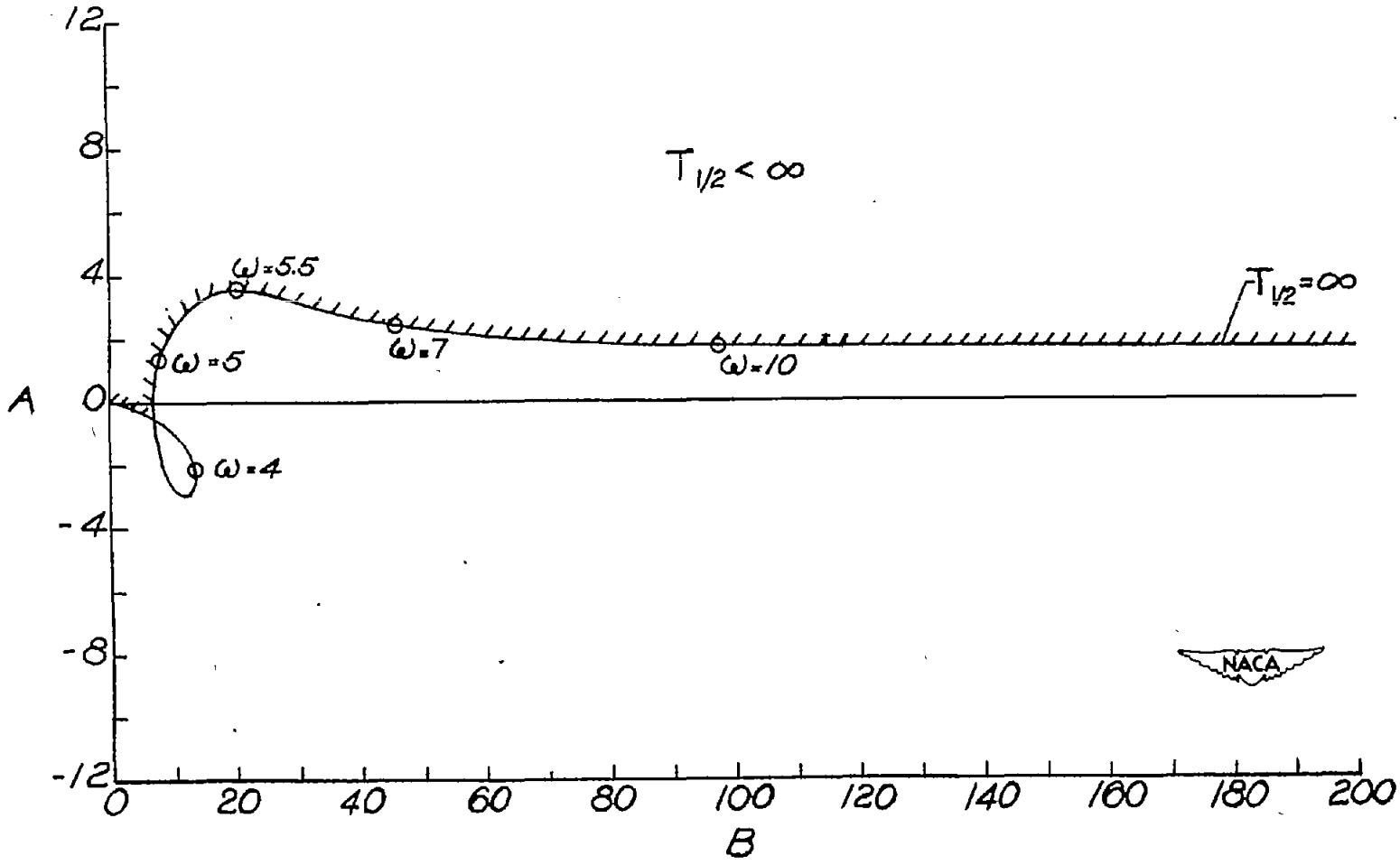

Figure 1.- Values of autopilot parameters A and B for which a neutrally damped oscillation will occur in the lateral motion. Three degrees of lateral freedom; K = 0.086 deg/deg/sec. Values of ω in radians per second are given at representative points.

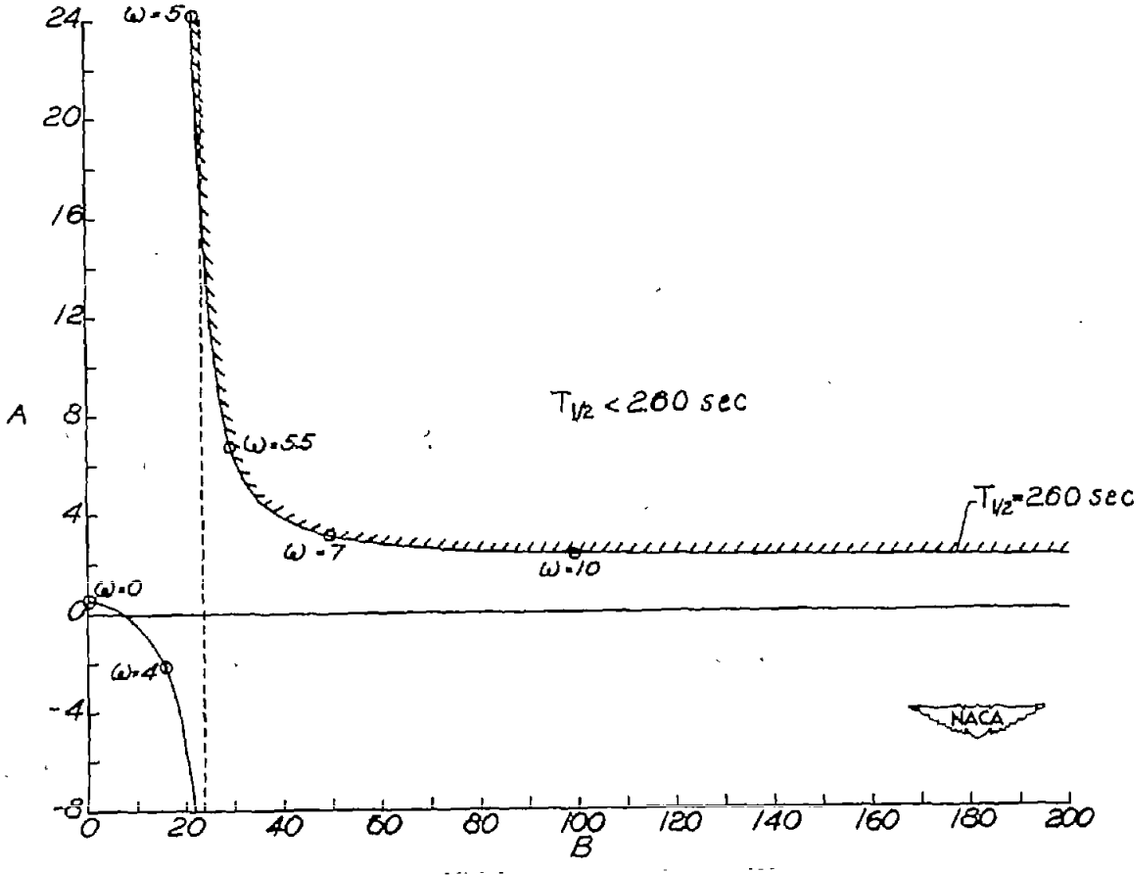

Figure 2.- Values of autopilot parameters A and B for which an oscillation will occur in the lateral motion with damping equal to that of the natural Dutch roll oscillation. Three degrees of lateral freedom; K = 0.086 deg/deg/sec. Values of ω in radians per second are given at representative points. The dashed line indicates the value of B corresponding to the airplane frequency.

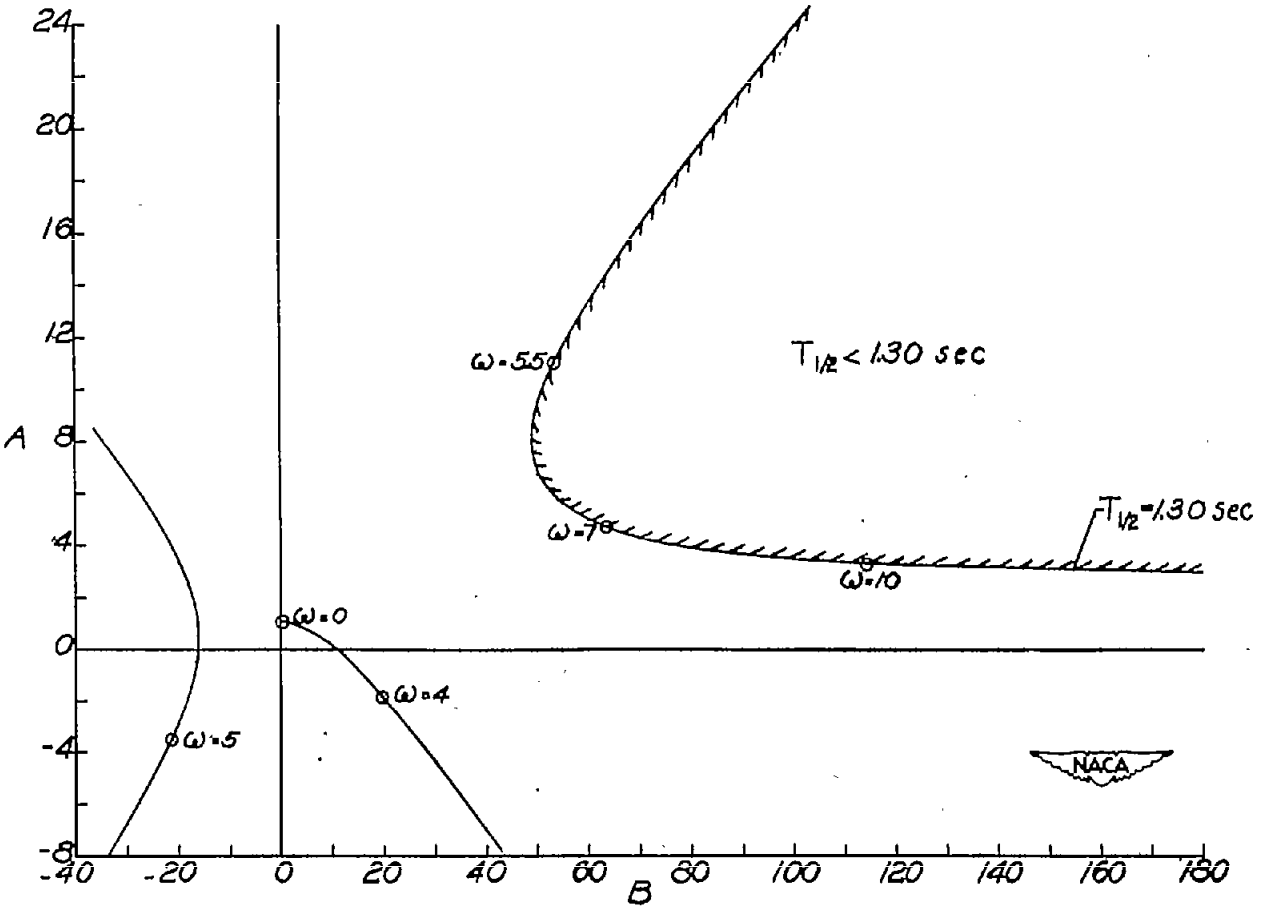

Figure 3.- Values of autopilot parameters A and B for which an oscillation will occur in the lateral motion with $T_{1/2}$ = 1.3 seconds, a typical damping value between the airplane damping and the critical damping. Three degrees of lateral freedom; K = 0.086 deg/deg/sec. Values of ω in radians per second are given at representative points.

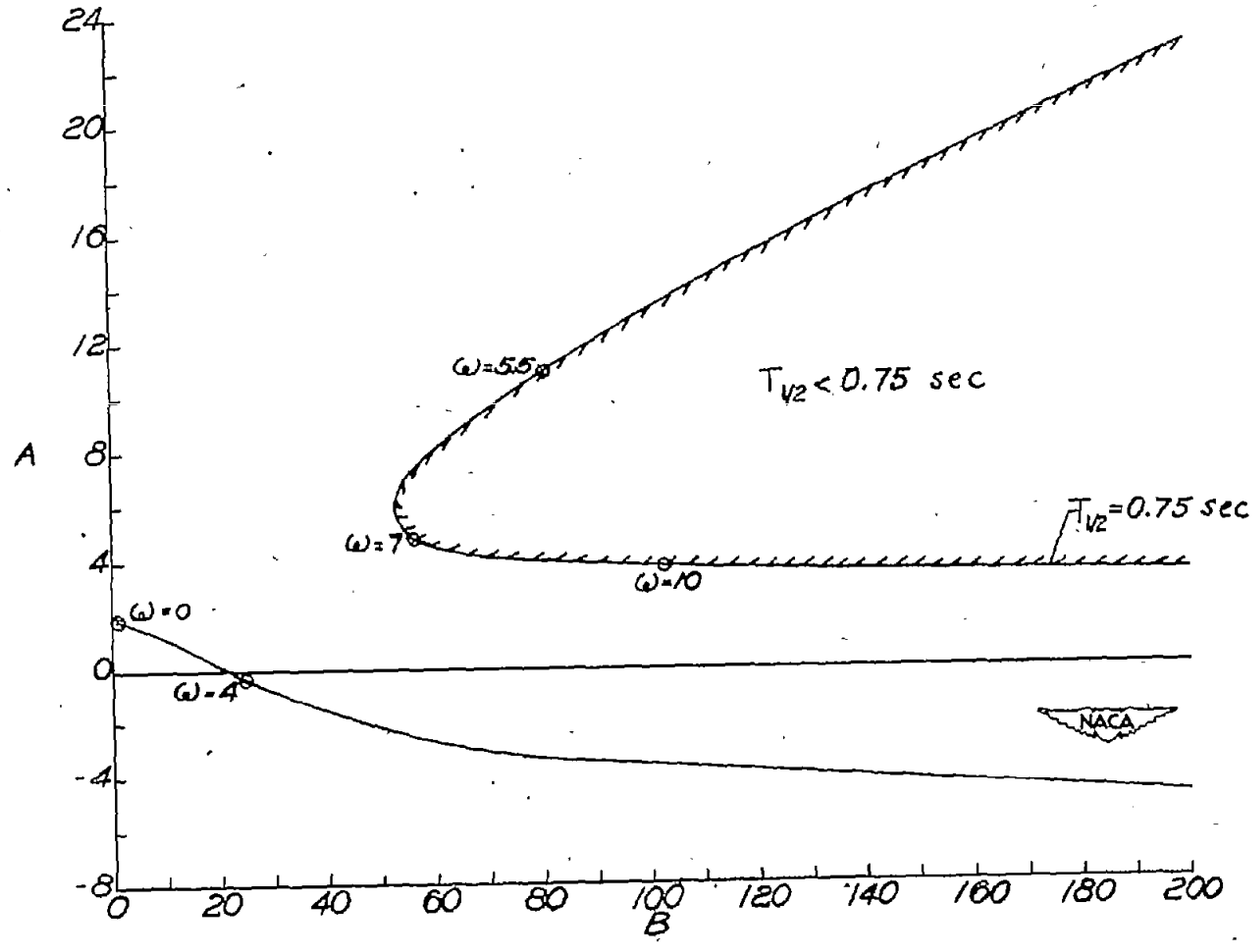

Figure 4.- Values of autopilot parameters A and B for which an oscillation will occur in the lateral motion with $T_{1/2} = 0.75$ second, the critical damping. Three degrees of lateral freedom; K = 0.086 deg/deg/sec. Values of ω in radians per second are given at representative points.

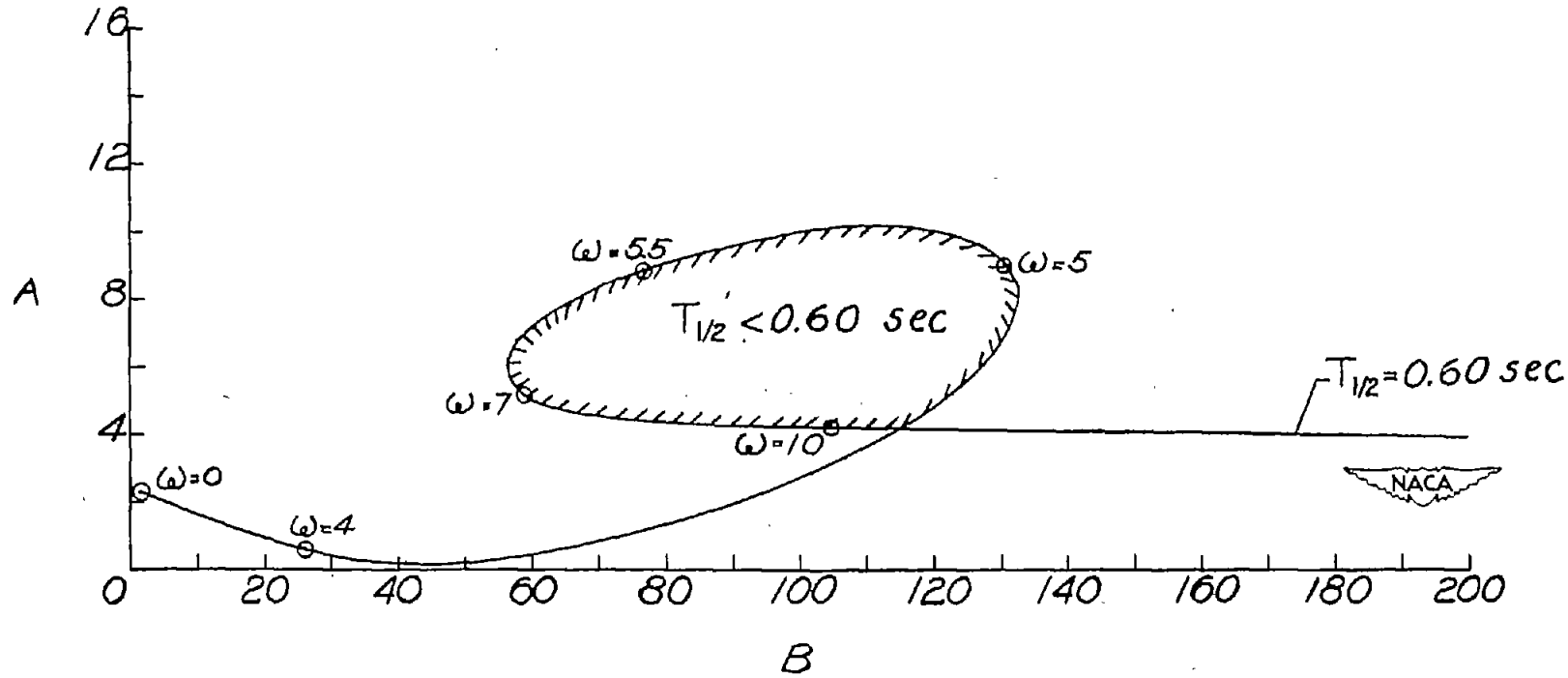

Figure 5.- Values of autopilot parameters A and B for which an oscillation will occur in the lateral motion with $T_{1/2}$ = 0.60 second, a typical damping curve for greater damping than the critical. Three degrees of lateral freedom; K = 0.086 deg/deg/sec. Values of ω in radians per second are given at representative points.

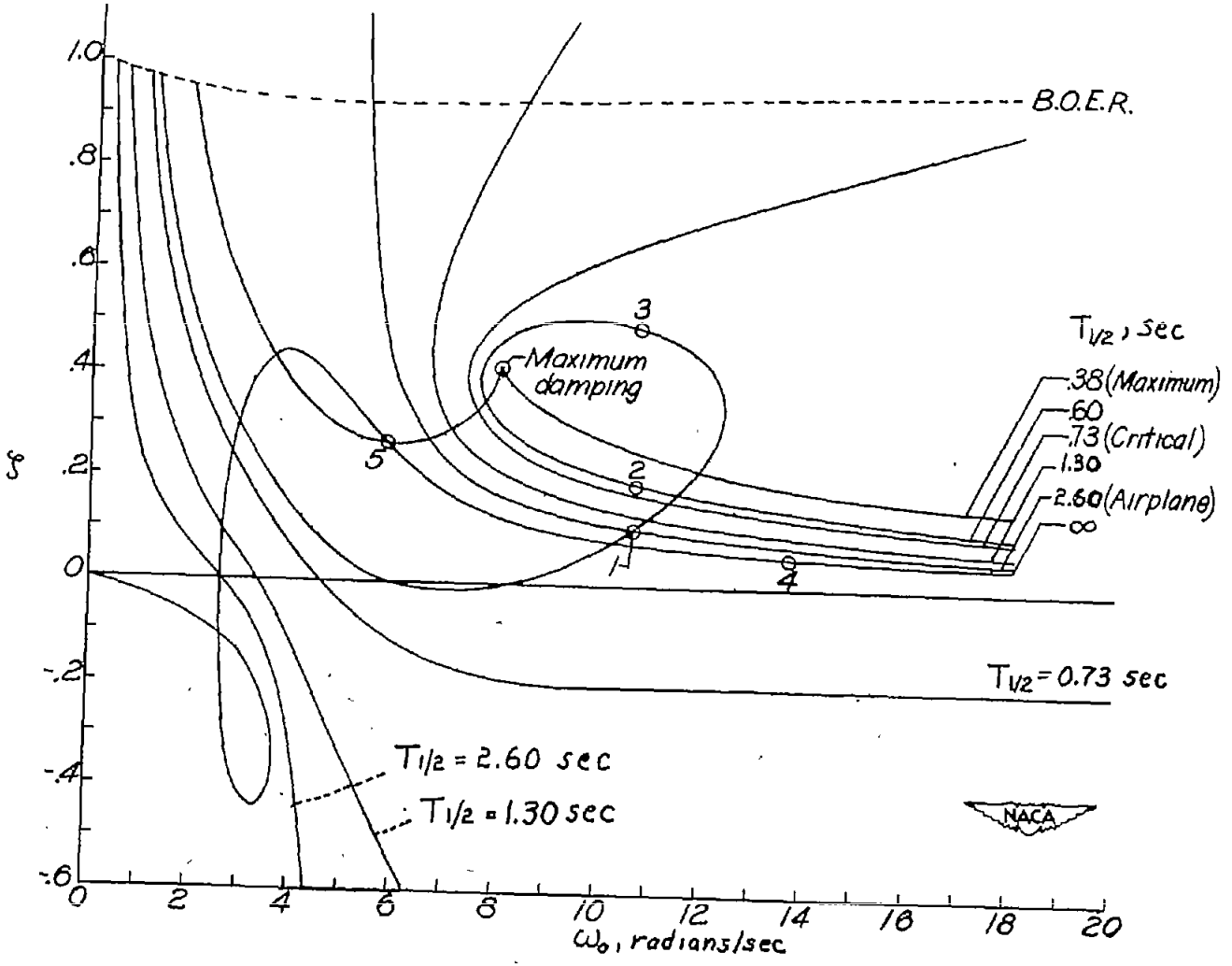

Figure 6.- Typical constant-damping curves in the $\zeta\omega_o$-plane showing the variation of the type of curve as the required damping increases. K = 0.086 deg/deg/sec. The dashed line is the boundary of equal roots.

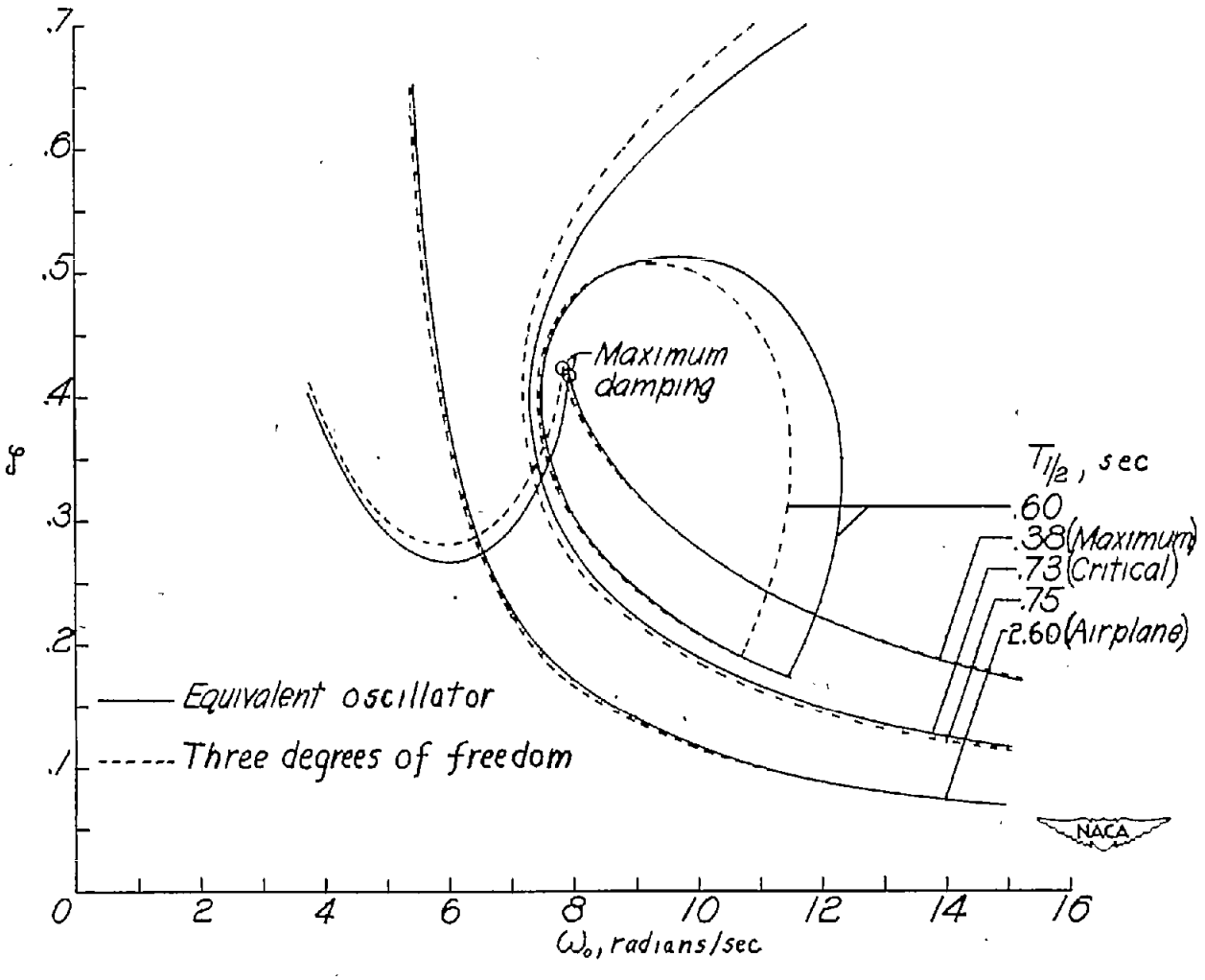

Figure 7.- Comparison of regions in the $\zeta\omega_o$-plane that insure various amounts of damping as calculated by the three-degree-of-freedom analysis and the equivalent-oscillator analysis. K = 0.086 deg/deg/sec.

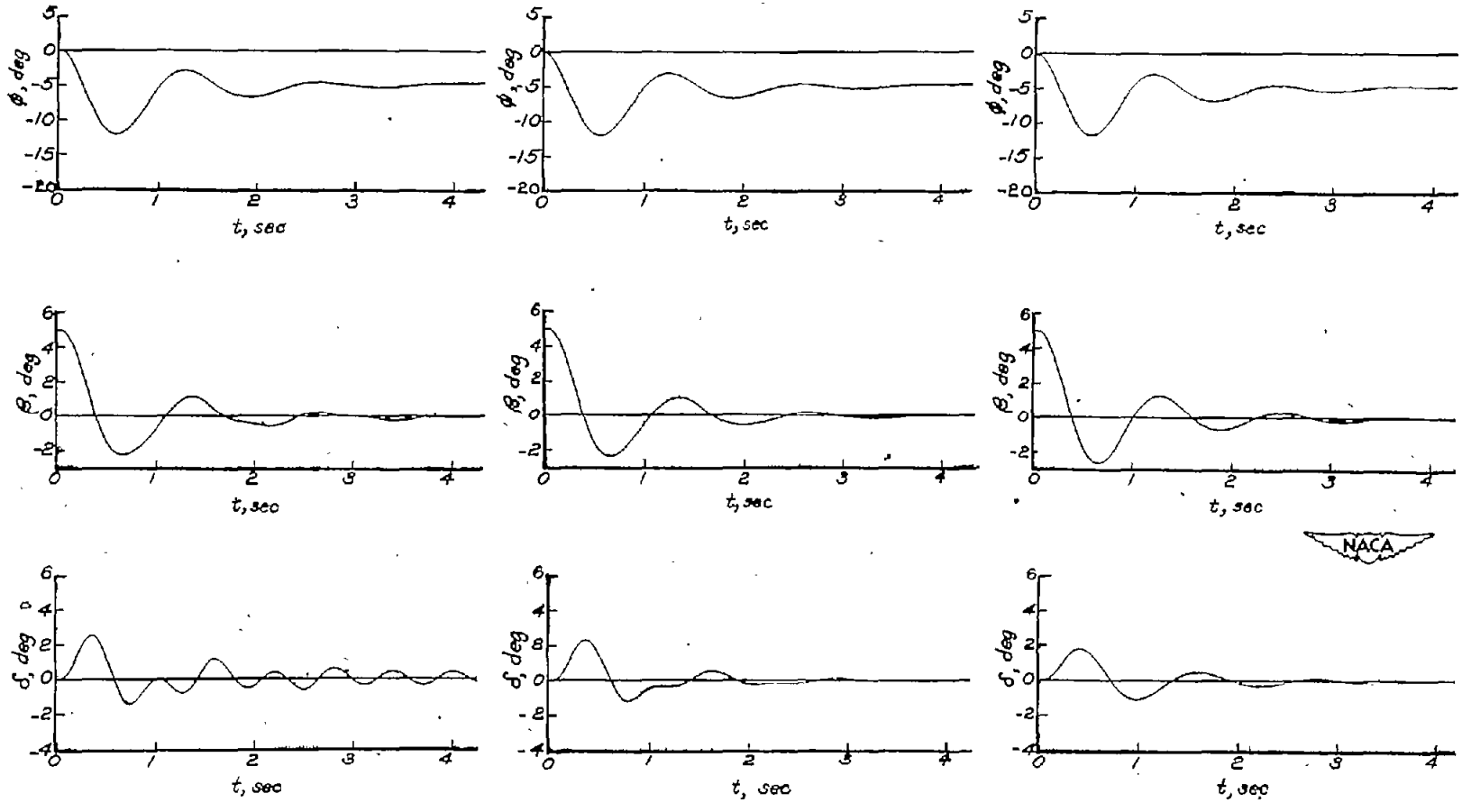

(a) K = 0.086 deg/deg/sec; ω_o = 10.66 radians per second; ζ = 0.11.

(b) K = 0.086 deg/deg/sec; ω_o = 10.66 radians per second; ζ = 0.1945.

(c) K = 0.086 deg/deg/sec; ω_o = 10.66 radians per second; ζ = 0.503.

Figure 8.- Comparison of motions with three different autopilots whose characteristics lie on a curve for $T_{1/2}$ = 0.60 second (corresponding to points 1, 2, and 3 in fig. 6).

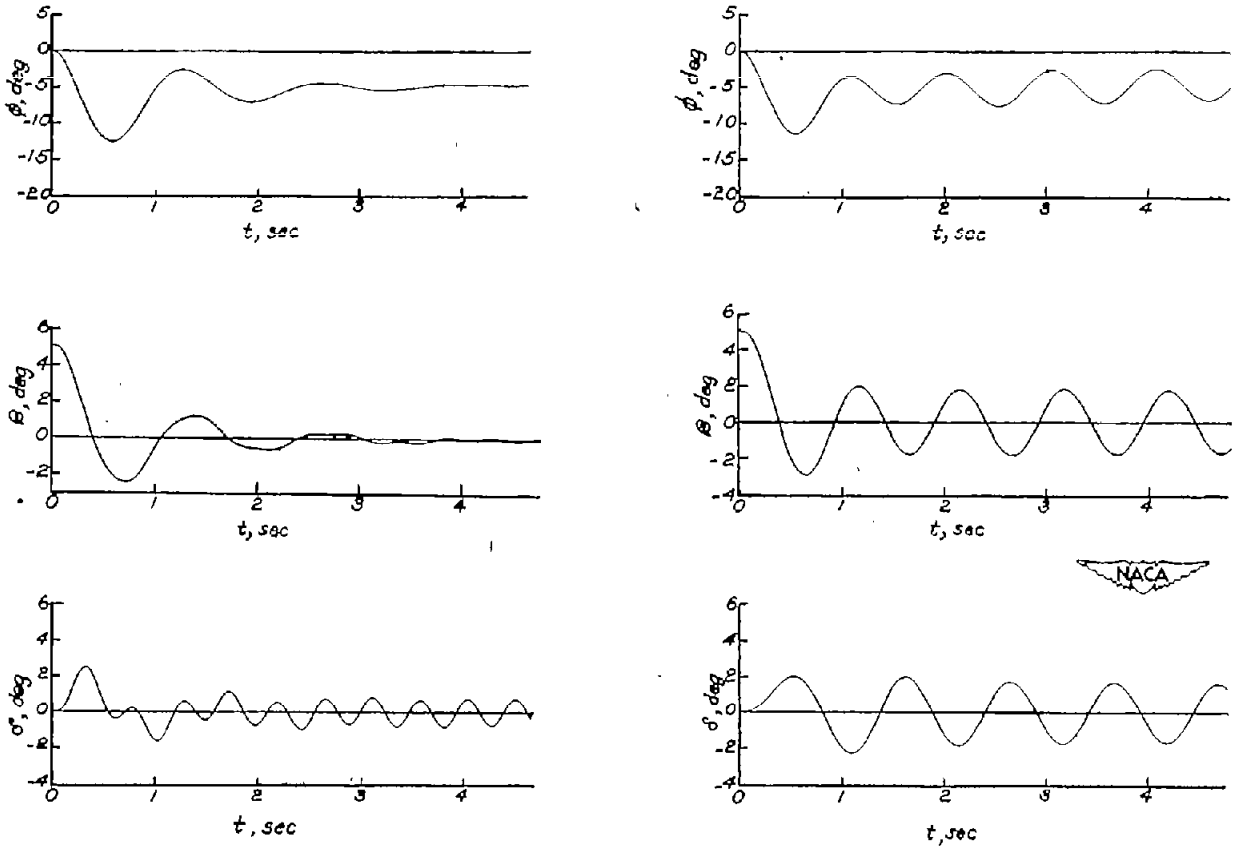

(a) K = 0.086 deg/deg/sec; ω_o = 13.65 radians per second; ζ = 0.0574.

(b) K = 0.086 deg/deg/sec; ω_o = 5.85 radians per second; ζ = 0.26.

Figure 9.- Comparison of motions with two different autopilots whose characteristics lie on a curve for $T_{1/2} = \infty$ (corresponding to points 4 and 5 in fig. 6).

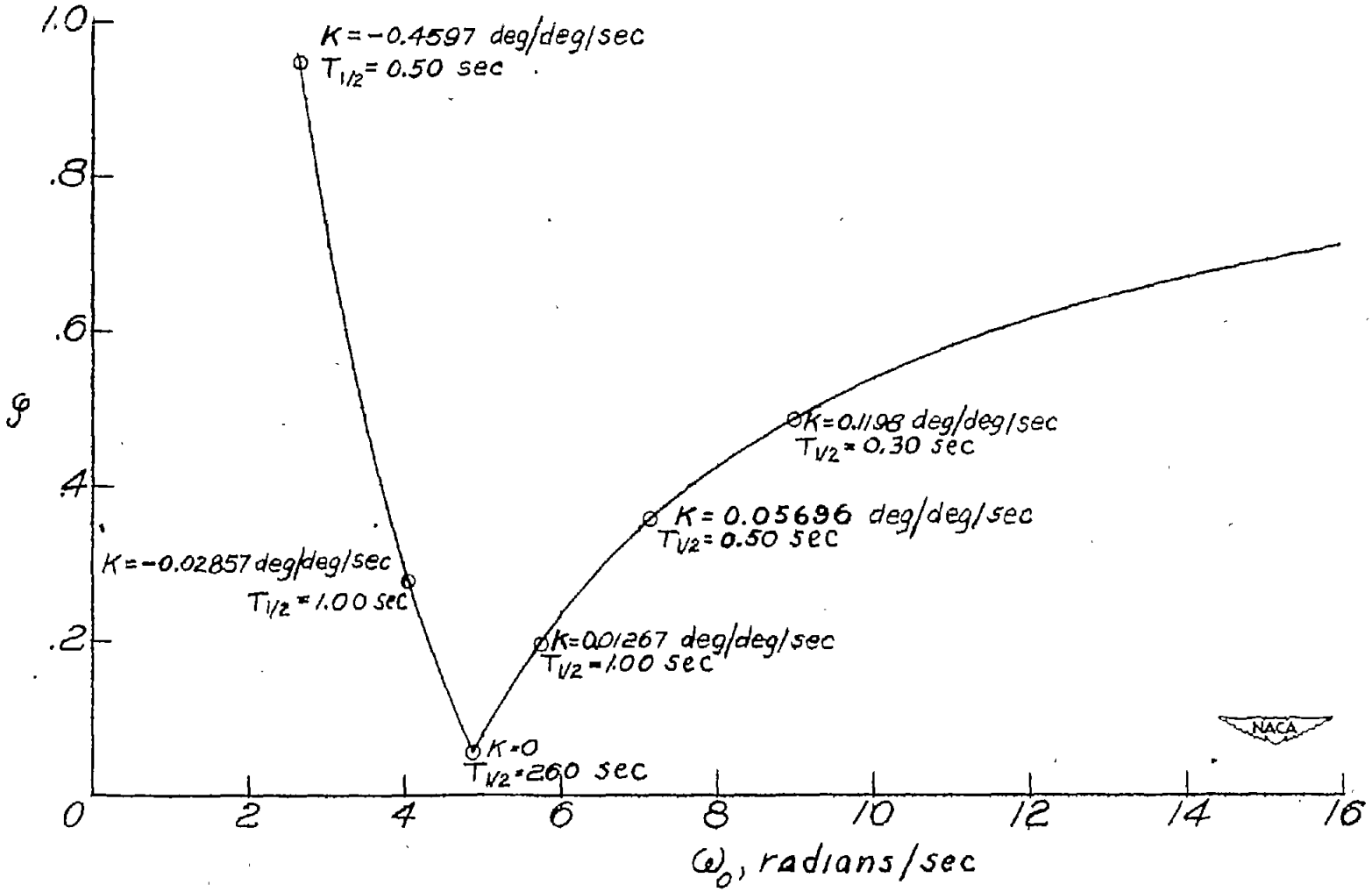

Figure 10.- Variation of optimum points in the $\zeta\omega_o$-plane for varying autopilot gearing ratio.

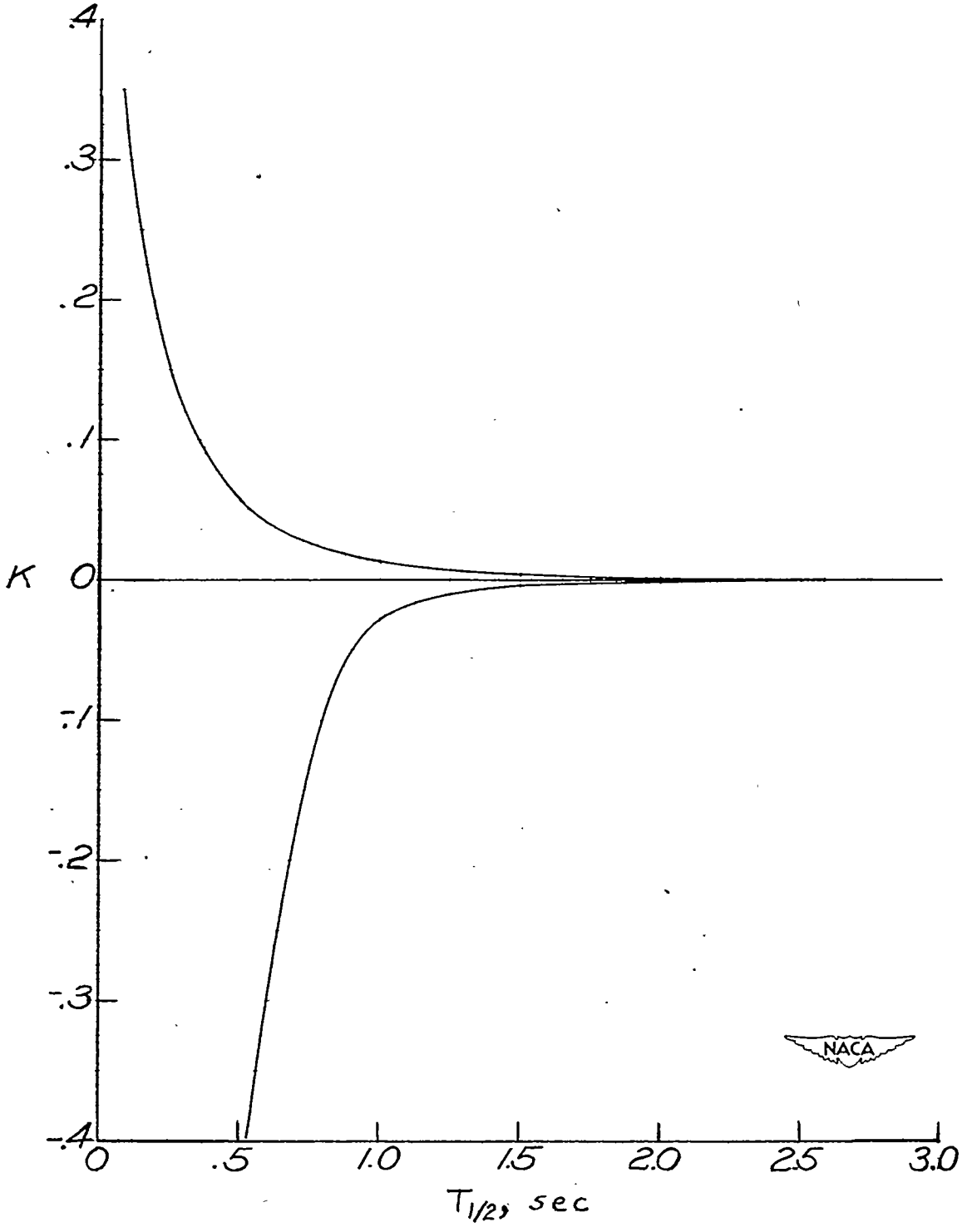

Figure 11.- Values of autopilot gearing ratio necessary to obtain a given damping as the maximum damping.

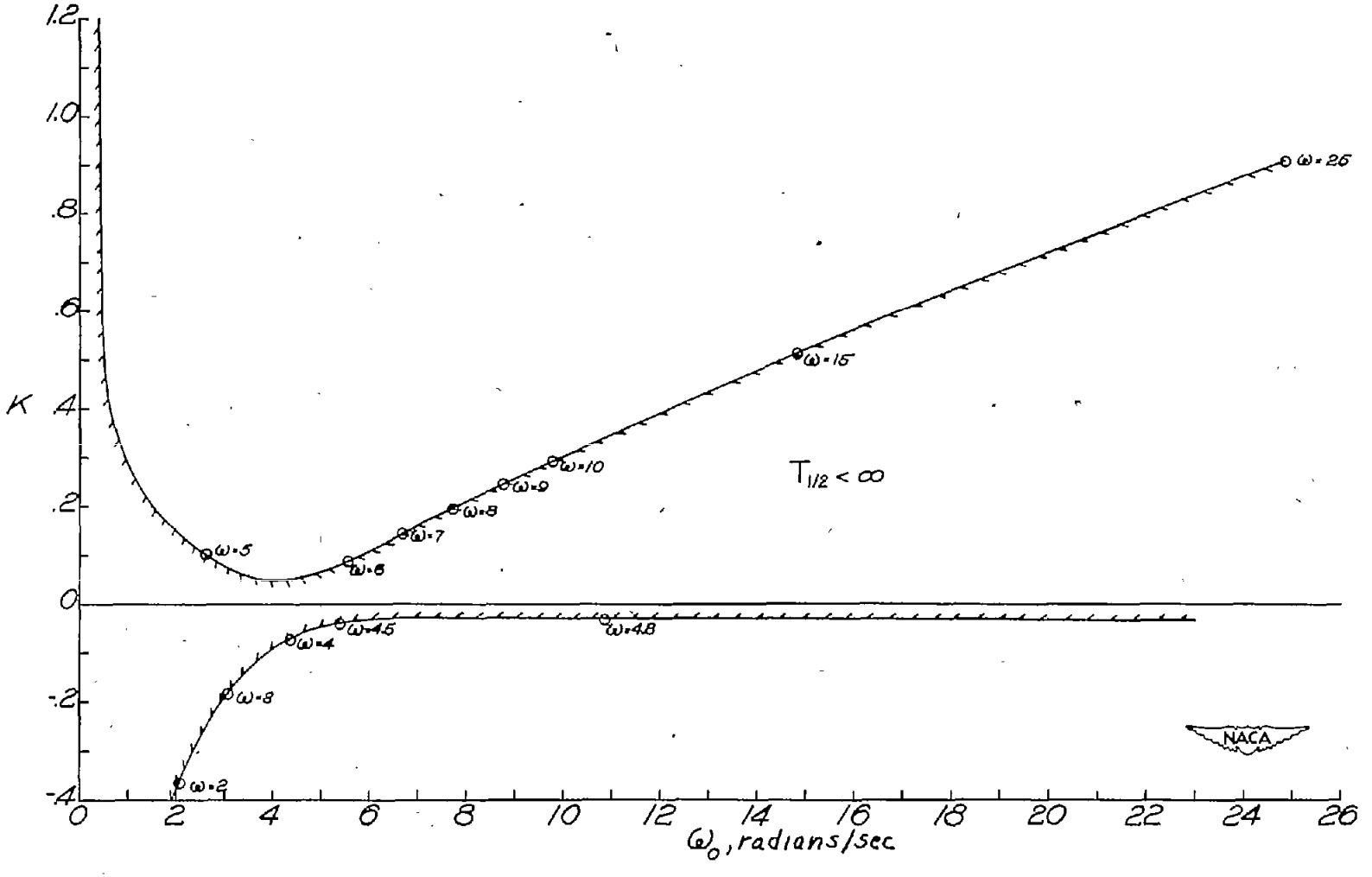

Figure 12.- Values of autopilot parameters K and ω_0 for which a neutrally damped oscillation will occur in the lateral motion. $\zeta = 0.3$. Values of ω in radians per second are given at representative points.

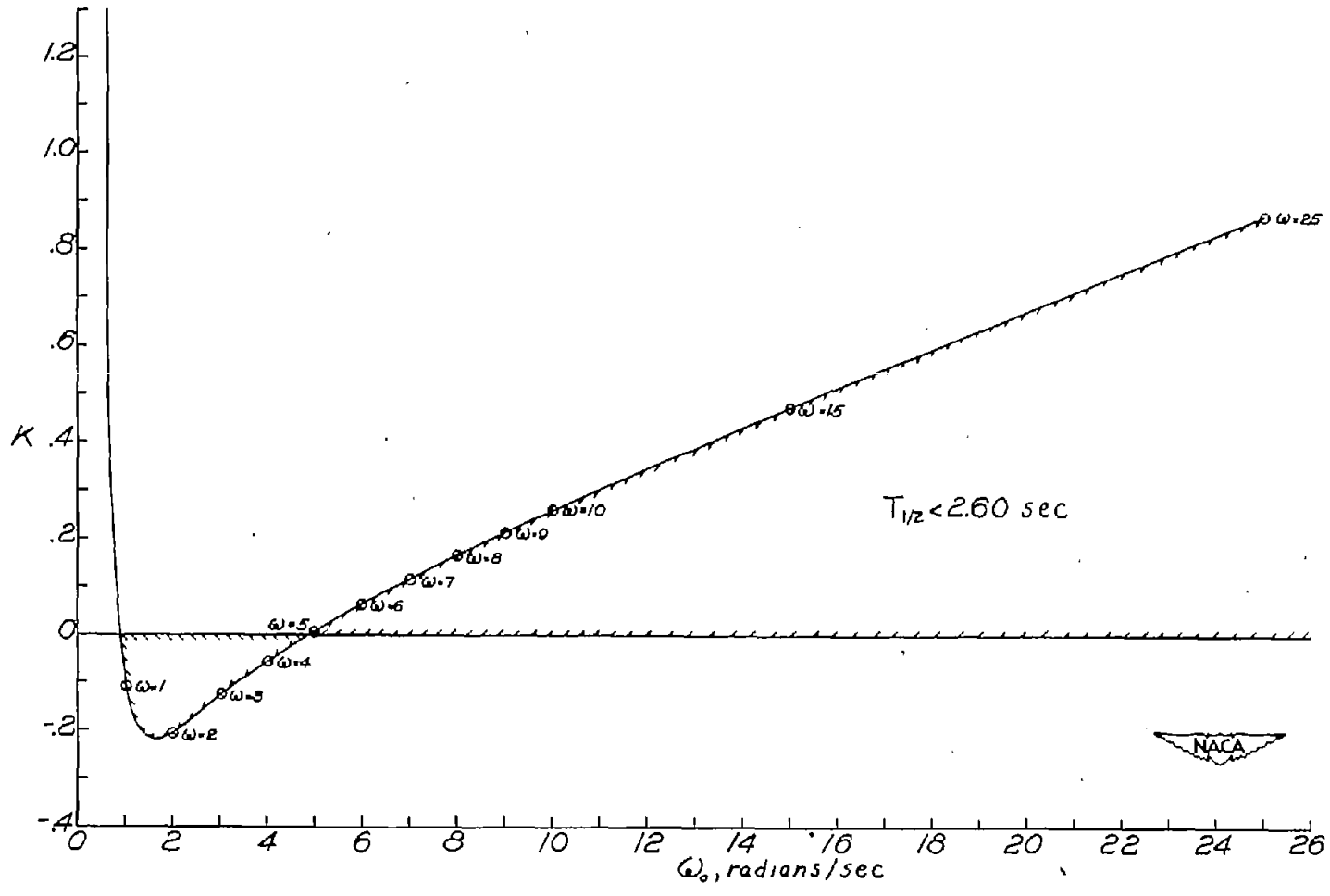

Figure 13.- Values of autopilot parameters K and ω_o for which an oscillation will occur in the lateral motion with damping equal to that of the natural Dutch roll oscillation. $\zeta = 0.3$. Values of ω in radians per second are given at representative points.

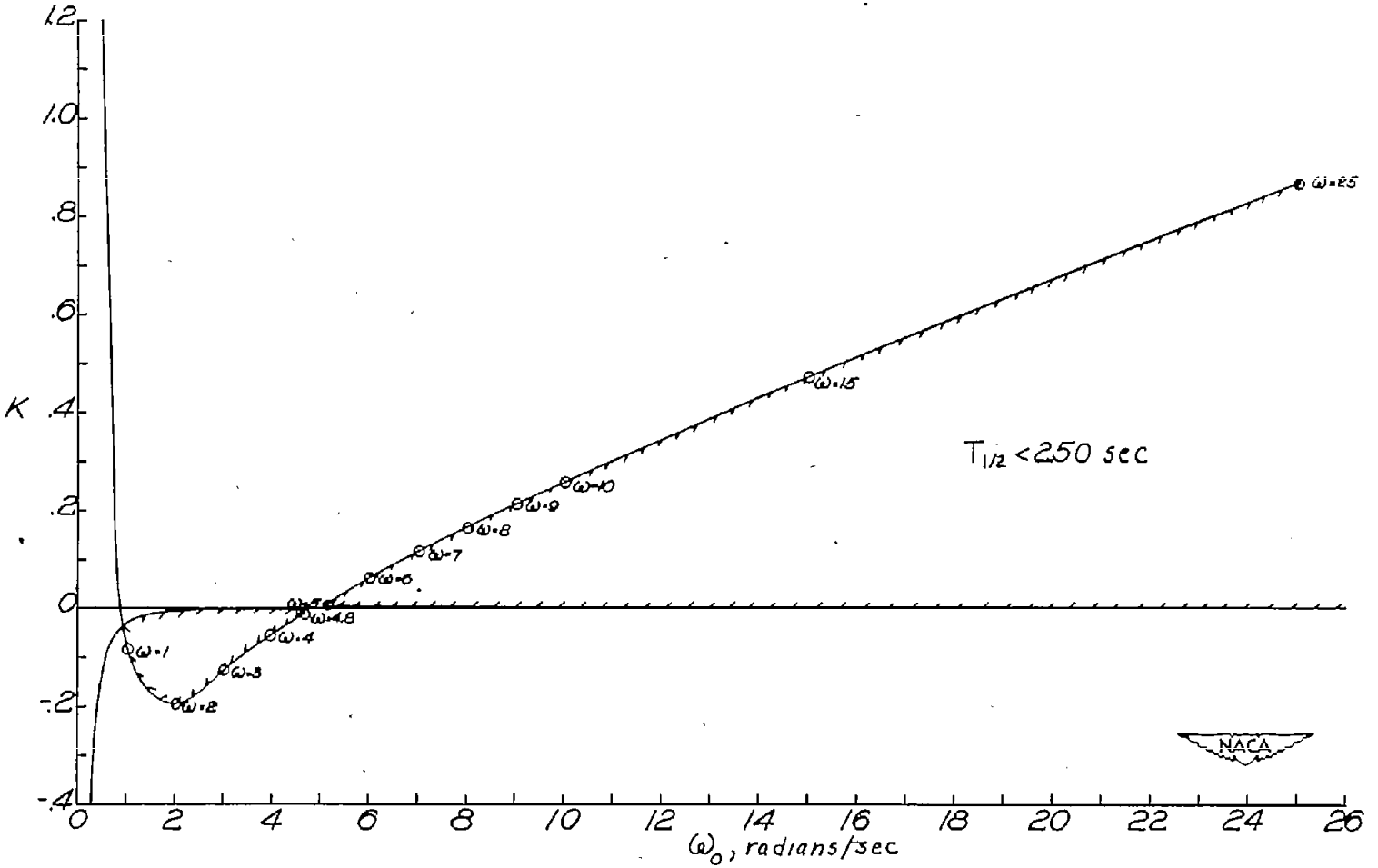

Figure 14.- Values of autopilot parameters K and ω_o for which an oscillation will occur in the lateral motion with damping slightly greater than that of the natural Dutch roll oscillation. $\zeta = 0.3$. Values of ω in radians per second are given at representative points.

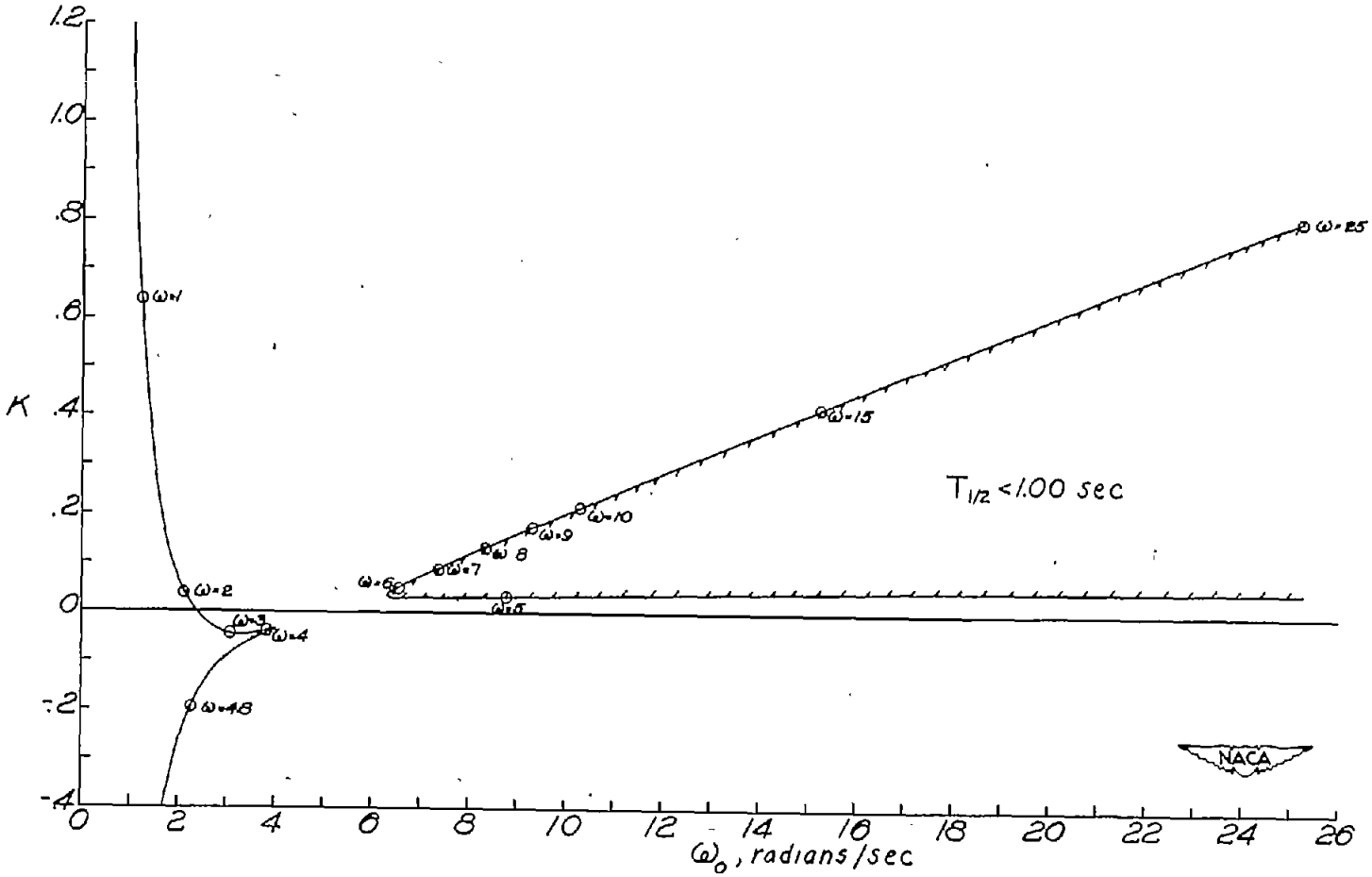

Figure 15.- Values of autopilot parameters K and ω_o for which an oscillation will occur in the lateral motion with $T_{1/2}$ = 1.00 second, the maximum damping for K < 0 with ζ = 0.3 (the value of ζ in this figure). Values of ω in radians per second are given at representative points.

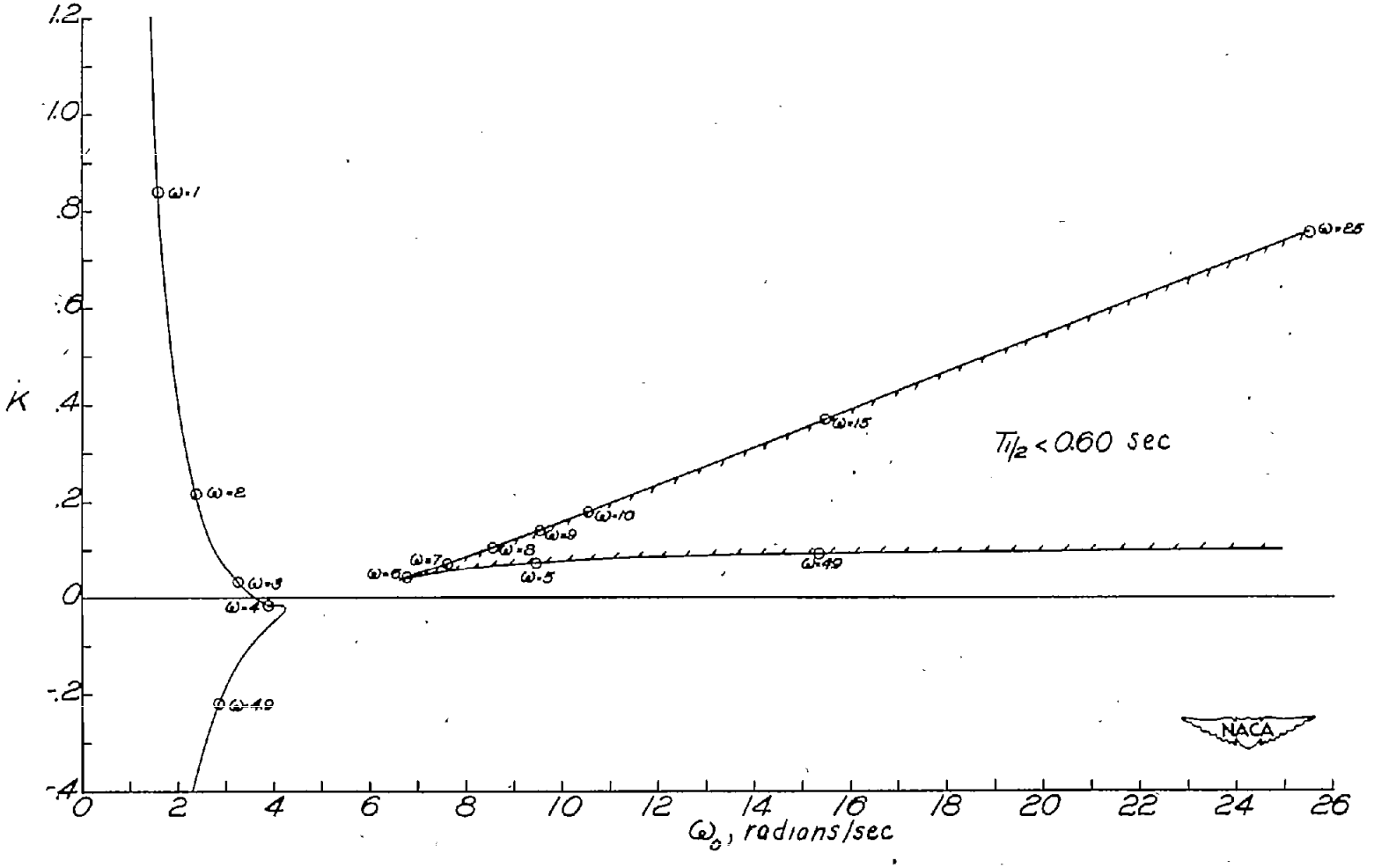

Figure 16.- Values of autopilot parameters K and ω_o for which an oscillation will occur in the lateral motion with $T_{1/2} = 0.60$ second. $\zeta = 0.3$. Values of ω in radians per second are given at representative points.

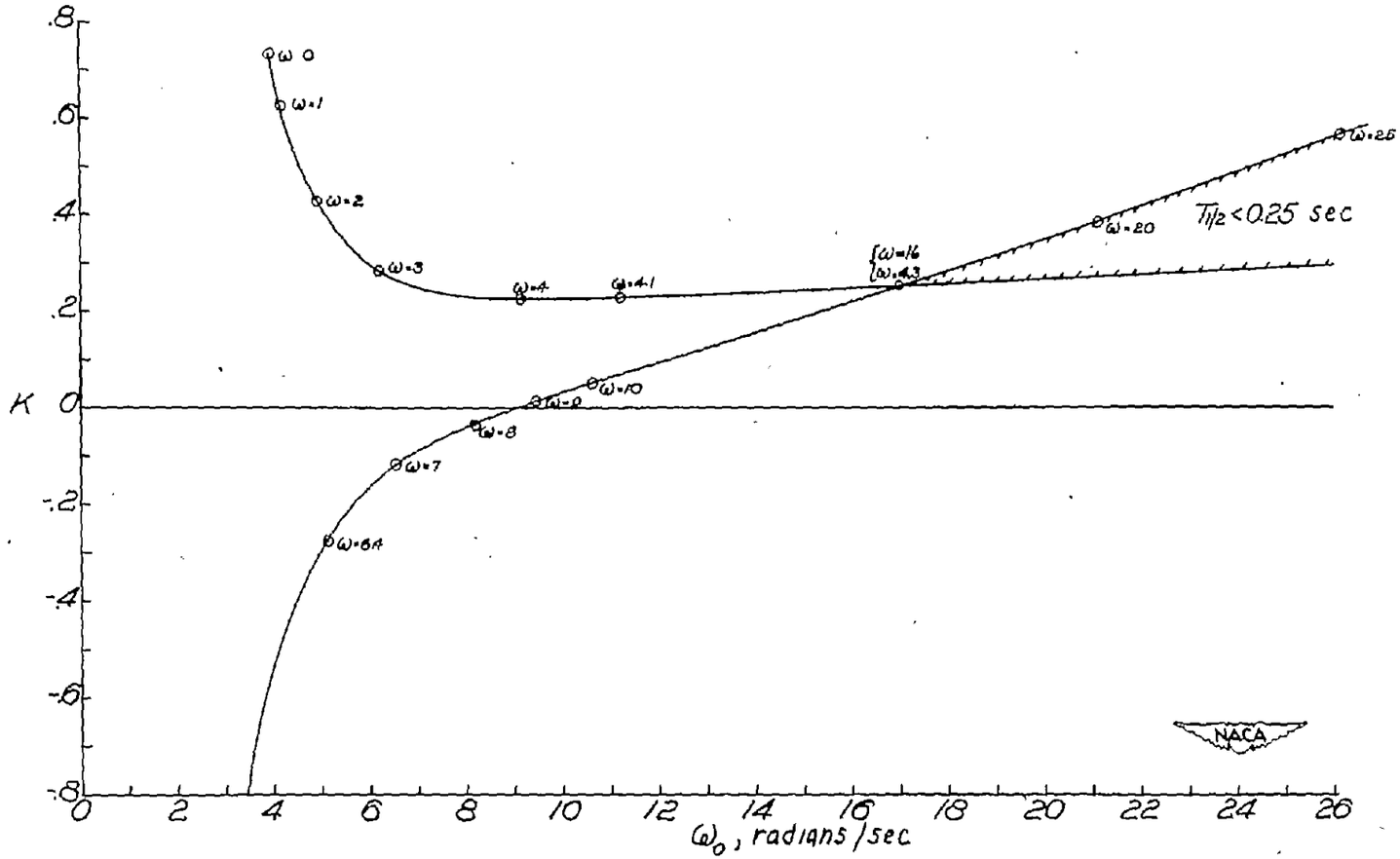

Figure 17.- A typical constant-damping boundary corresponding to a moderately high value of damping, for which a range of values of ω exists which cannot occur with this damping at any real value of ω_o. $\zeta = 0.3$. Values of ω in radians per second are given at representative points.

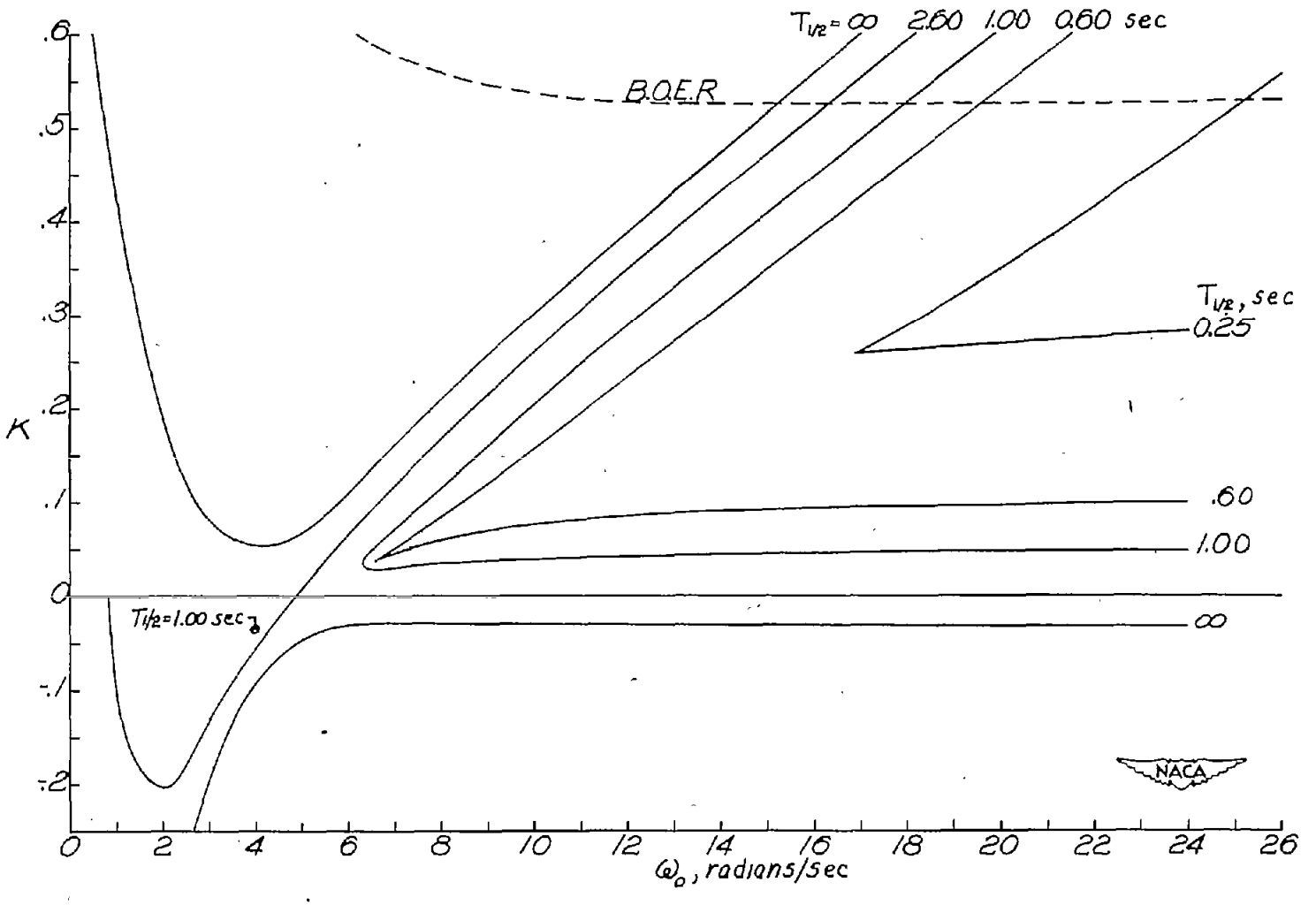

Figure 18.- Typical constant-damping curves in the $K\omega_o$-plane showing the variation in the type of boundary as the damping increases. $\zeta = 0.3$. The dashed line is the boundary of equal roots.

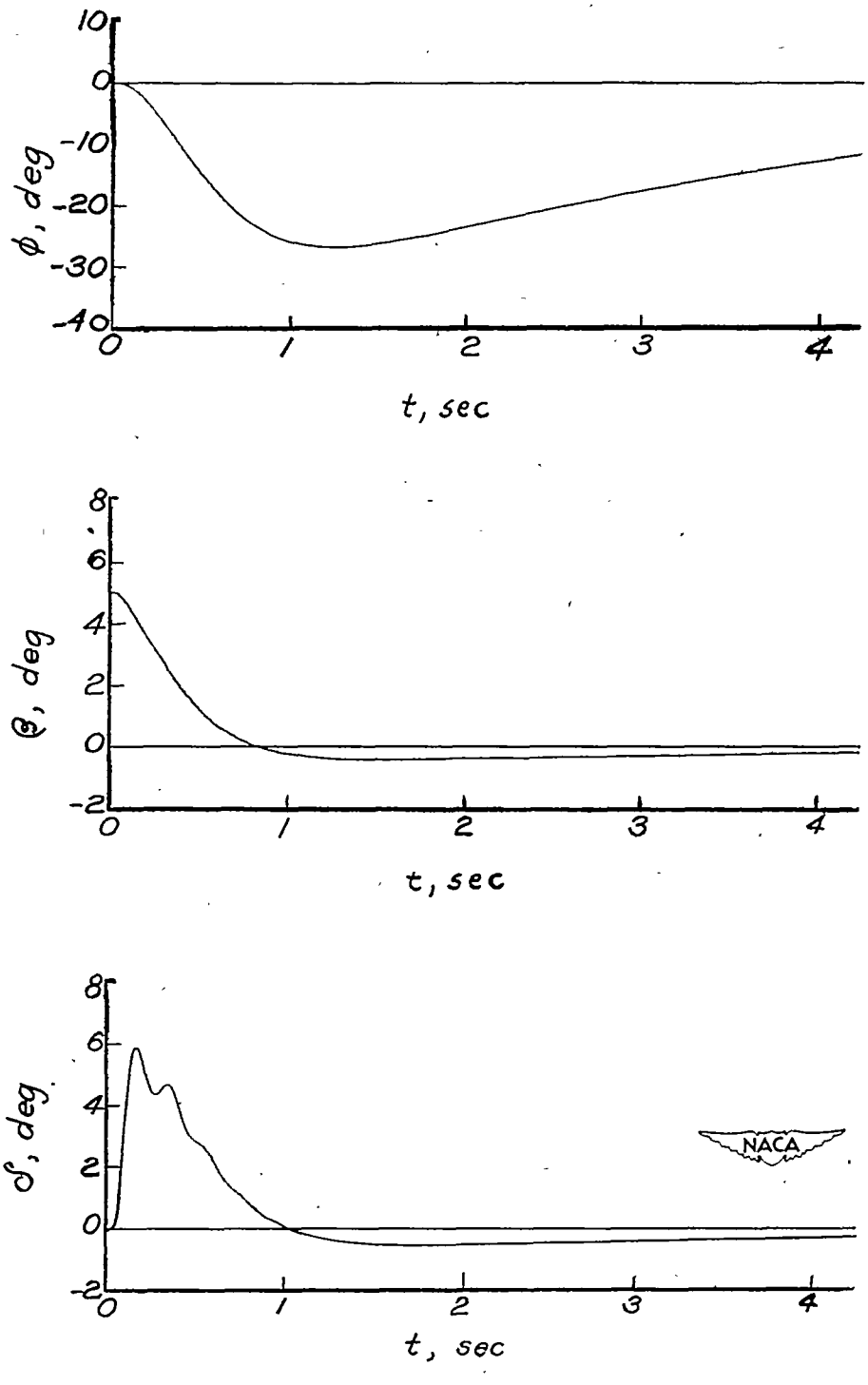

Figure 19.- Airplane and rudder motions with autopilot designed for maximum possible damping with $\zeta = 0.3$. K = 0.5386 deg/deg/sec; ω_o = 33.3 radians per second; $\zeta = 0.3$.

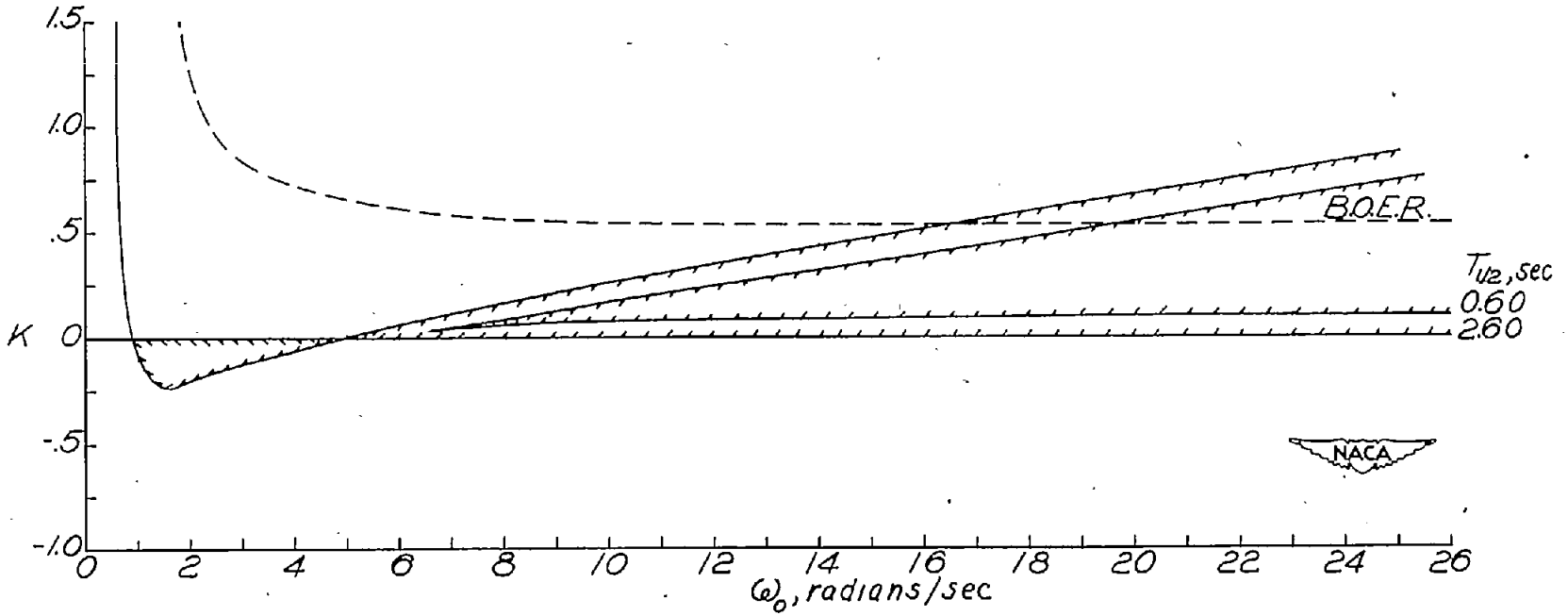

(a) $\zeta = 0.3$.

Figure 20.- Comparison of the boundary of equal roots, the airplane-damping region, and a typical increased-damping region in the $K\omega_o$-plane for values of $\zeta = 0.3$, 0.6, and 0.9.

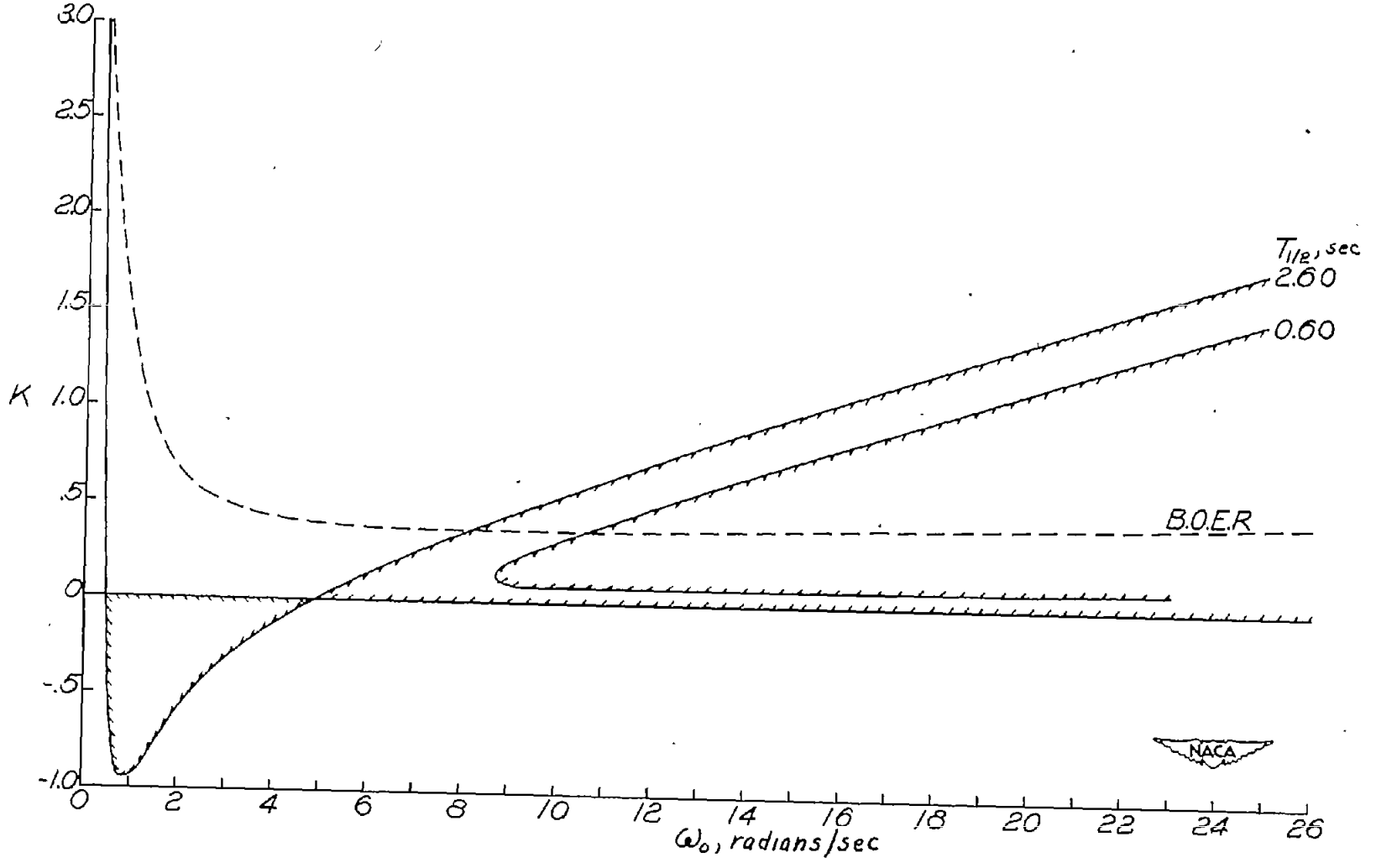

(b) $\zeta = 0.6$.

Figure 20.- Continued.

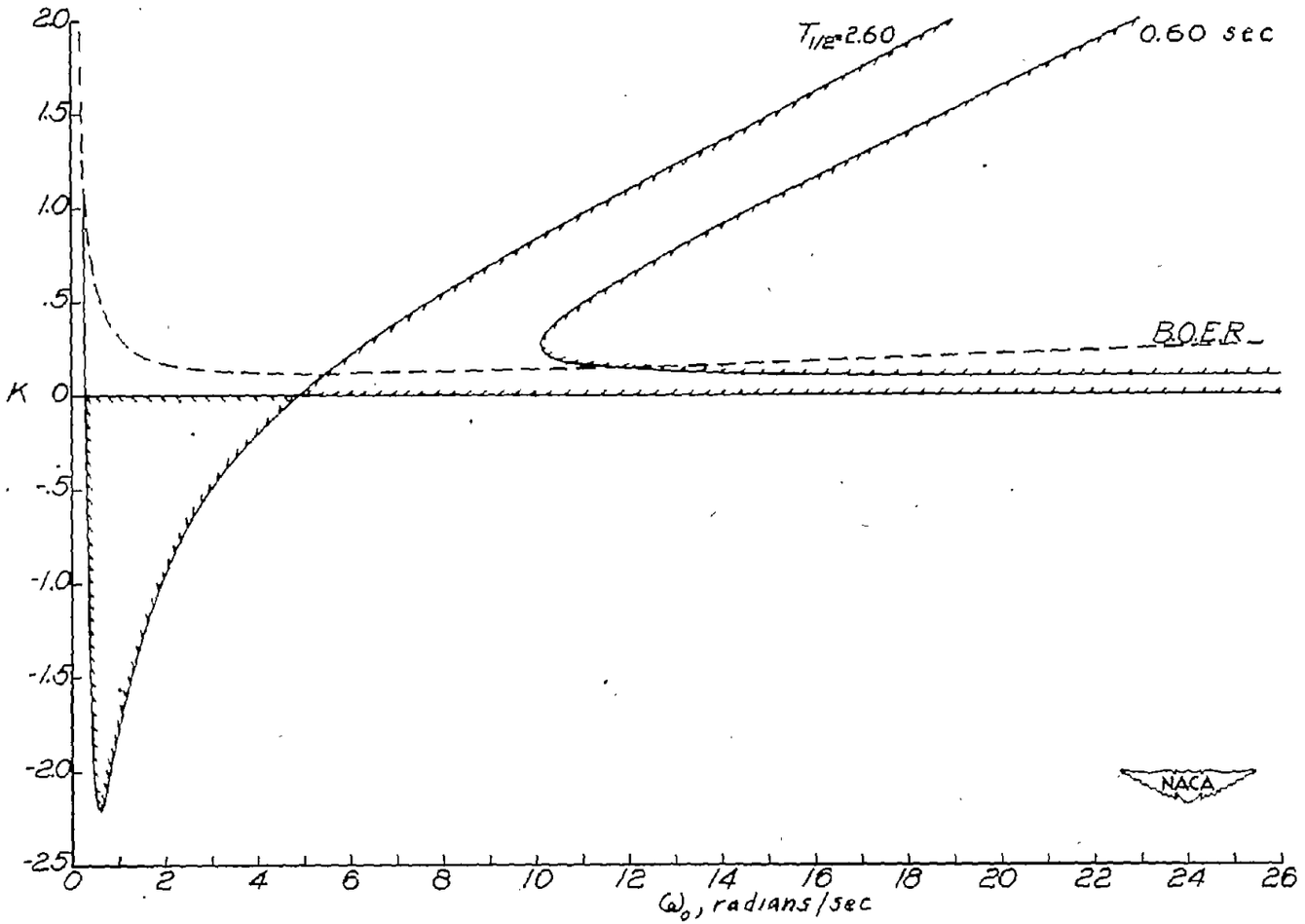

(c) $\zeta = 0.9$.

Figure 20.- Concluded.

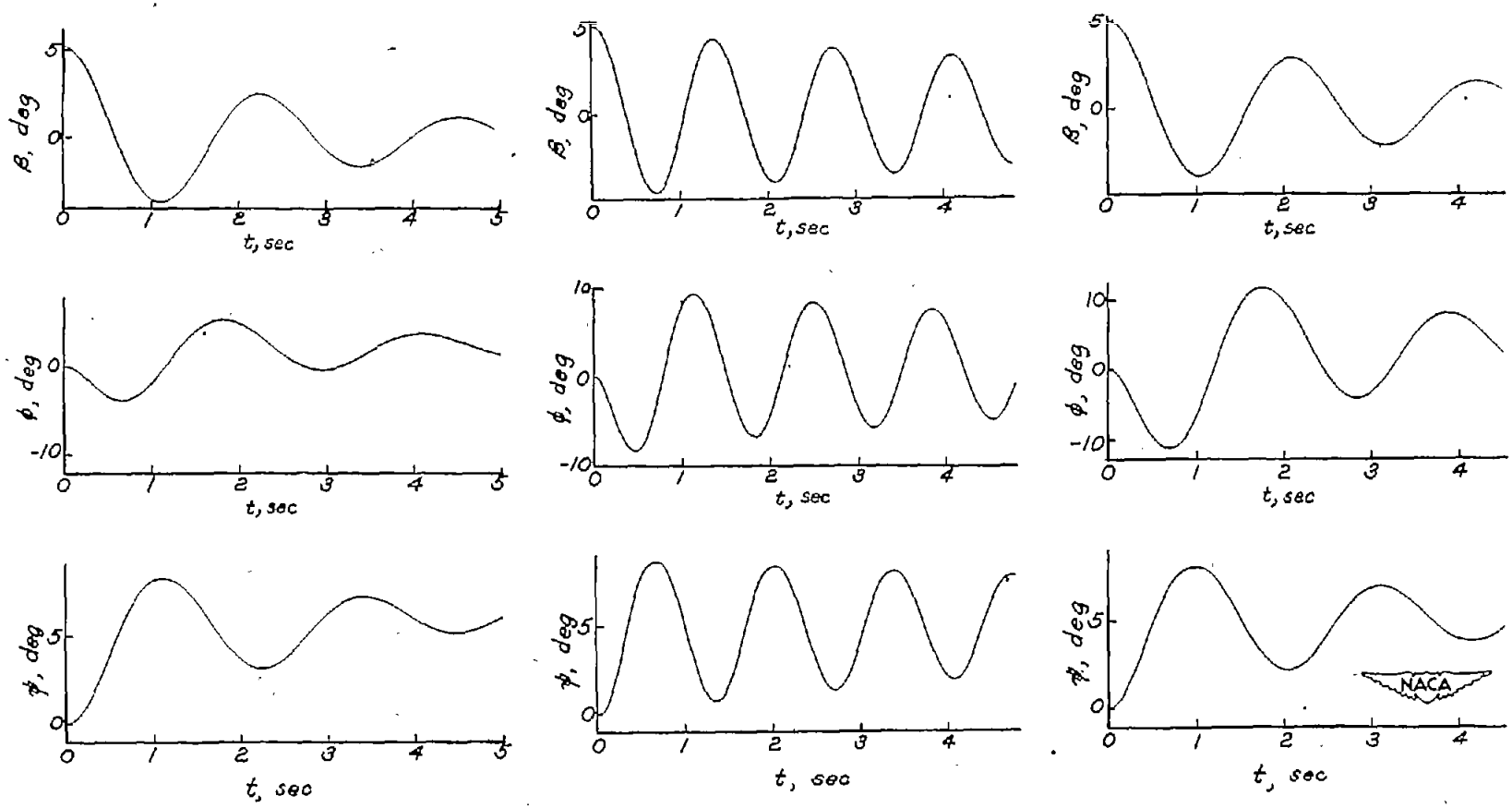

(a) Case I. (b) Case II. (c) Case III.

Figure 21.- Calculated motions for three flight conditions of the airplane subsequent to a 5° sideslip disturbance when no yaw damper is used.

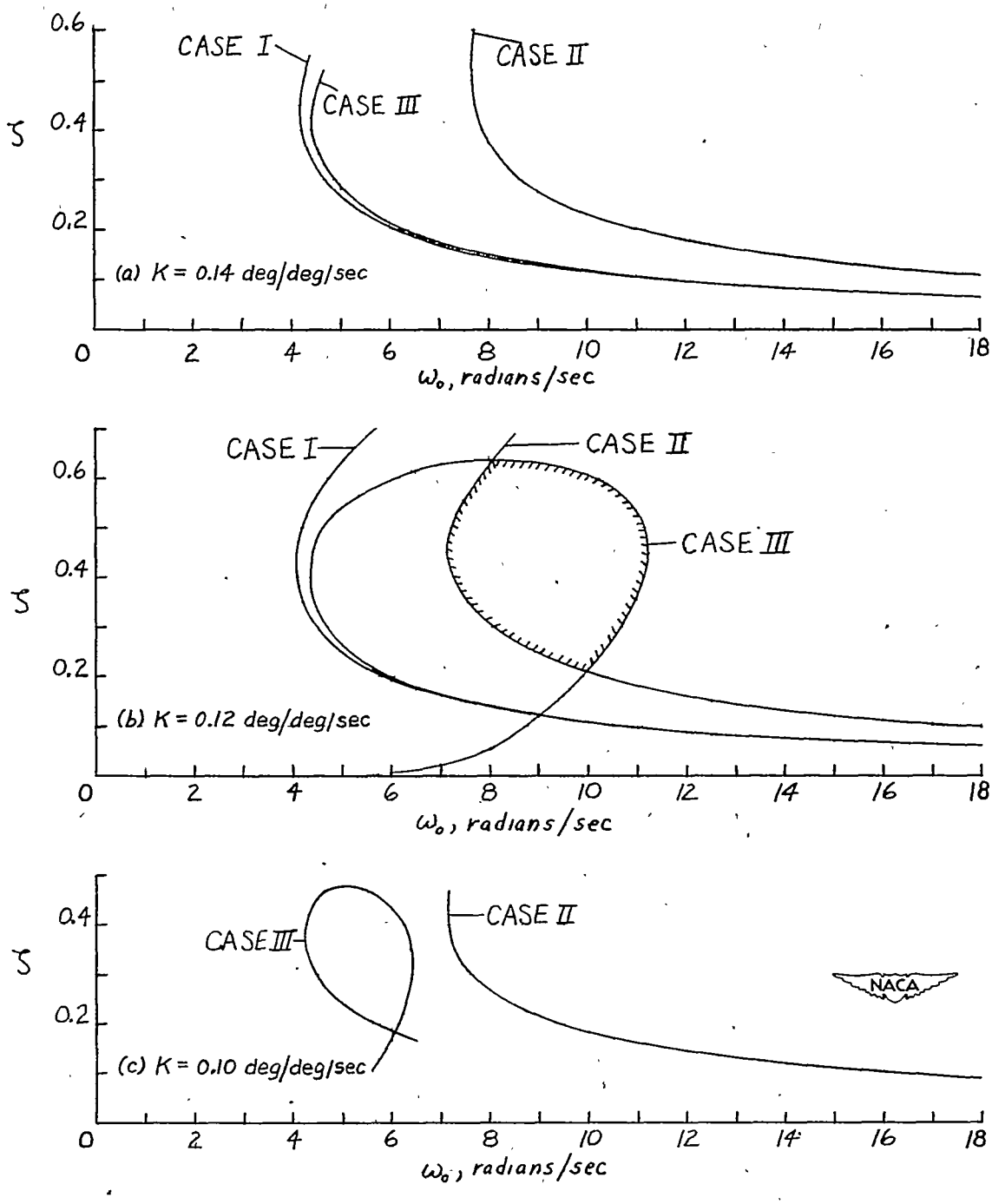

Figure 22.- Boundaries of the region where $T_{1/2} < 1.00$ second in the $\zeta\omega_o$-plane for three flight conditions of the airplane when a yaw damper with three different gearings is used.

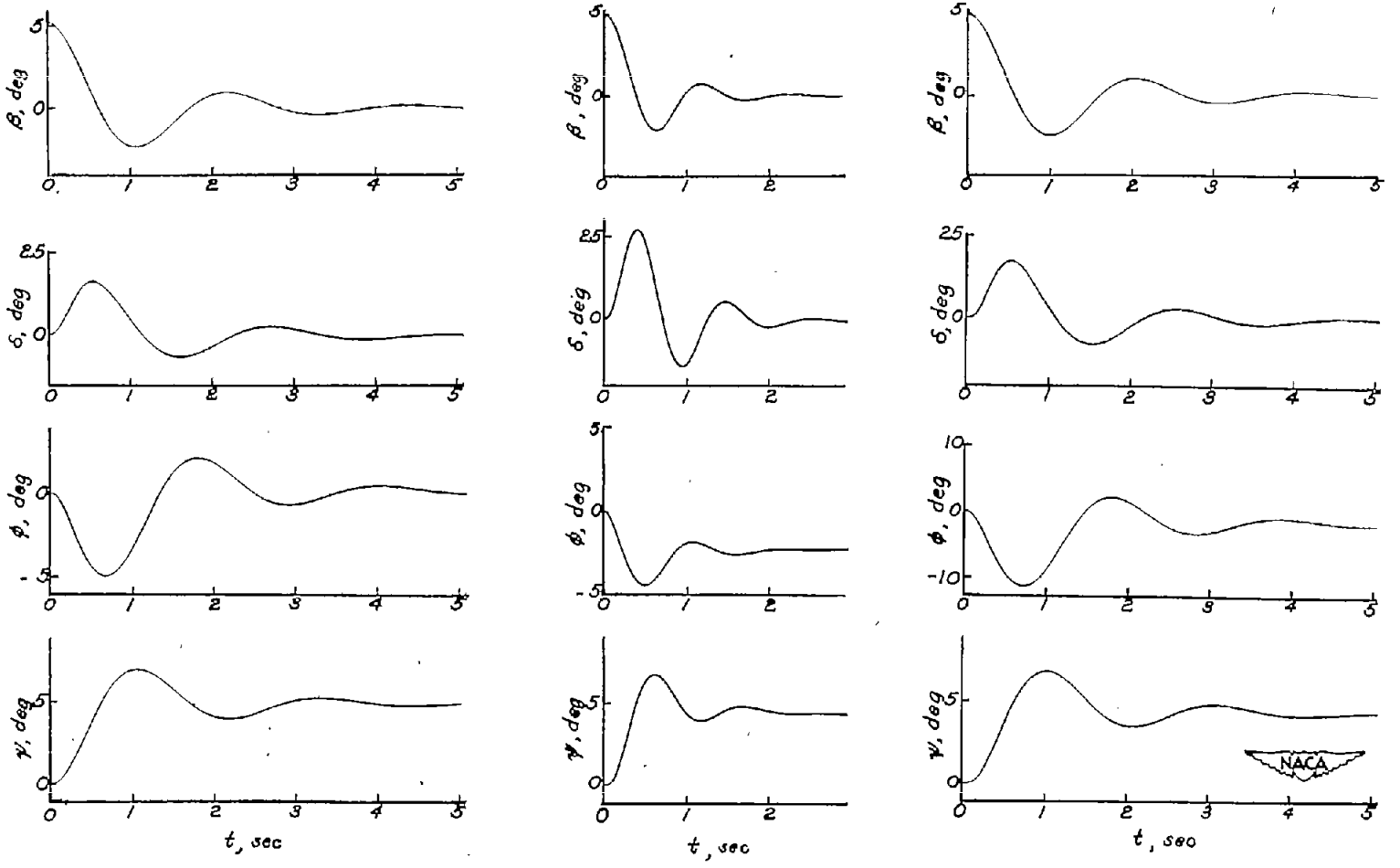

(a) Case I. (b) Case II. (c) Case III.

Figure 23.- Calculated motions for three flight conditions of the airplane subsequent to a 5° sideslip disturbance. Autopilot characteristics: $K = 0.14$ deg/deg/sec; $\zeta = 0.523$; $\omega_o = 9.49$ radians per second.

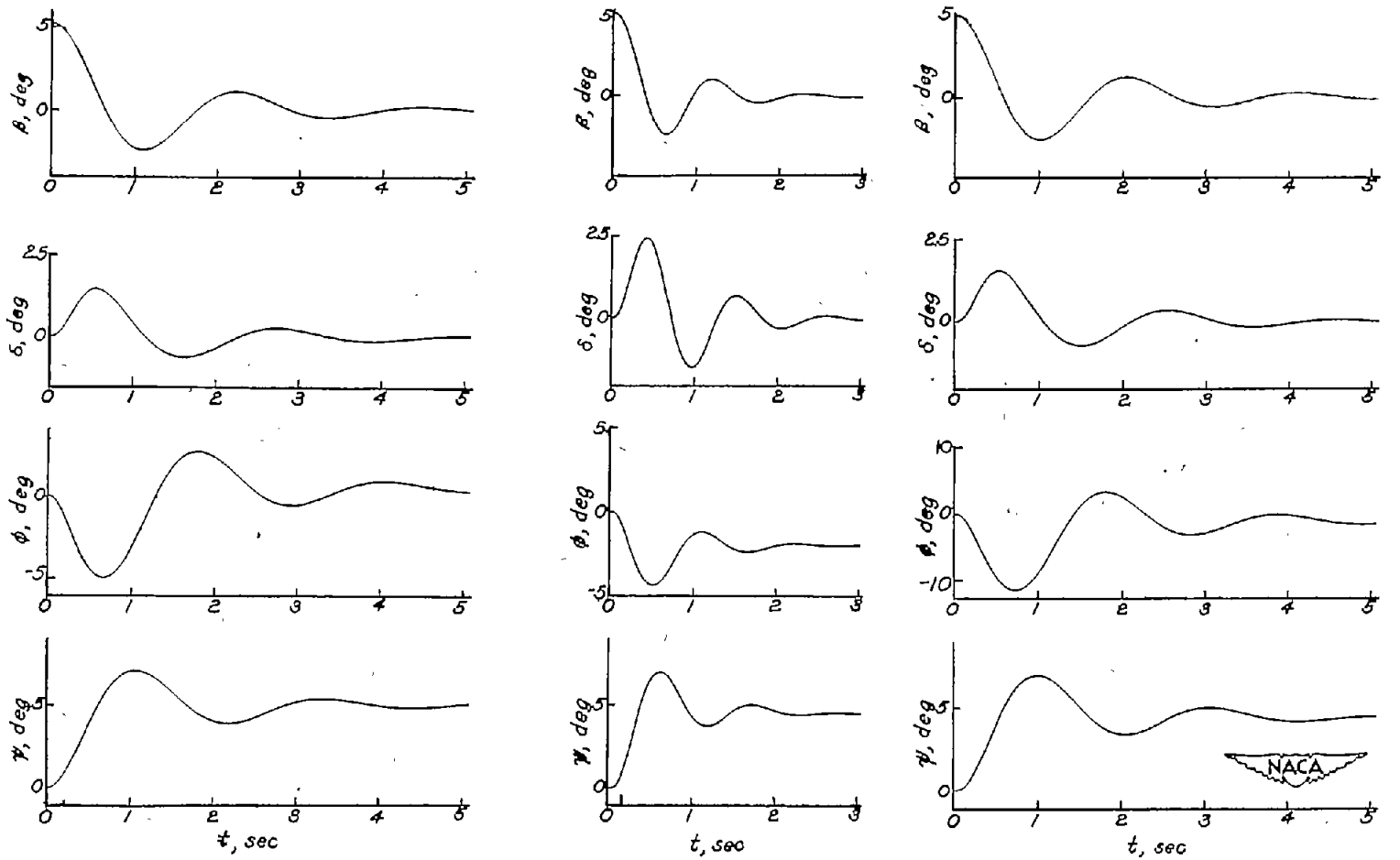

(a) Case I. (b) Case II. (c) Case III.

Figure 24.- Calculated motions for three flight conditions of the airplane subsequent to a 5° sideslip disturbance. Autopilot characteristics: $K = 0.12$ deg/deg/sec; $\zeta = 0.485$; $\omega_o = 8.81$ radians per second.

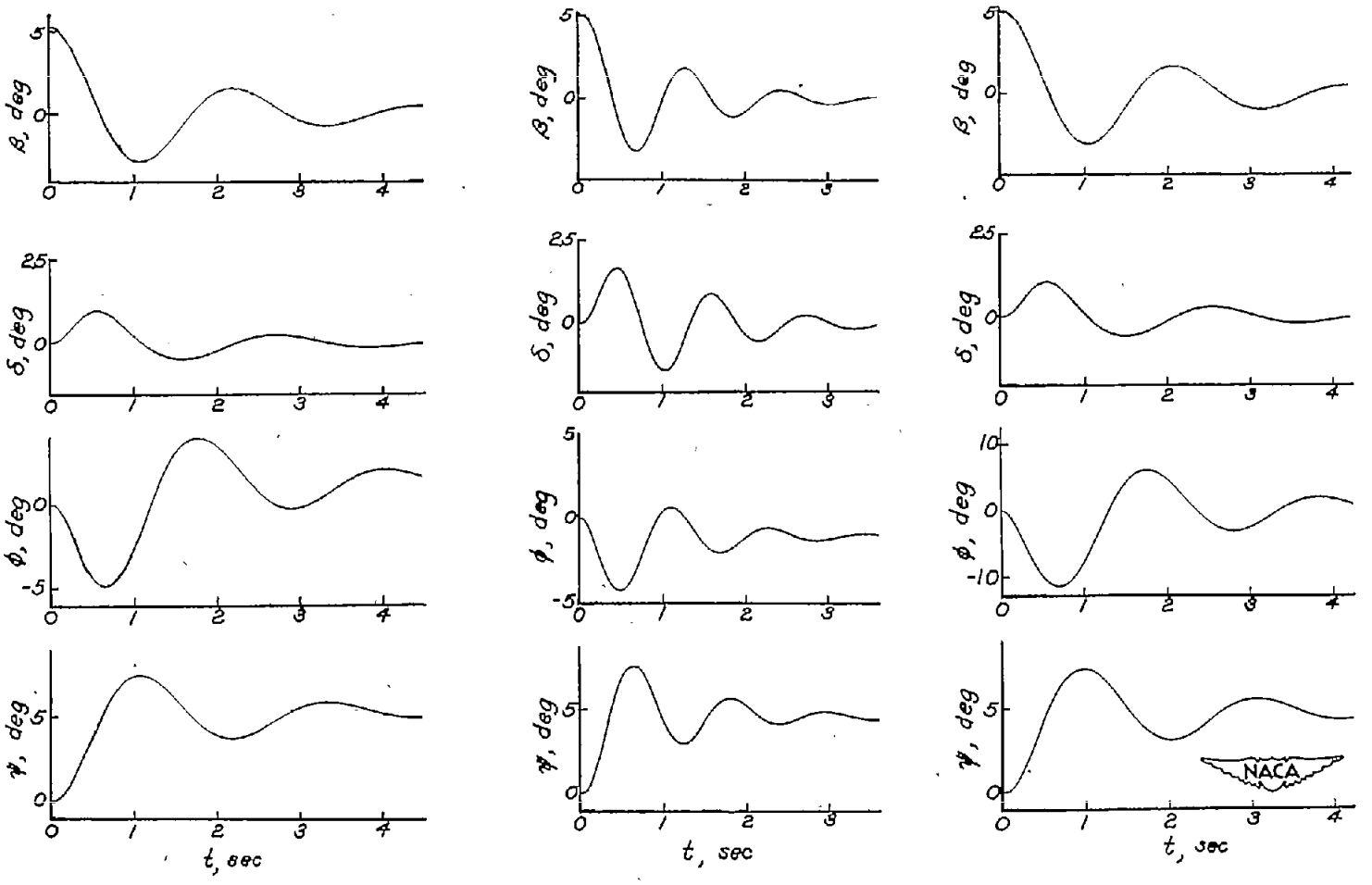

(a) Case I. (b) Case II. (c) Case III.

Figure 25.- Calculated motions for three flight conditions of the airplane subsequent to a 5° sideslip disturbance. Autopilot characteristics: K = 0.075 deg/deg/sec; ζ = 0.389; ω_o = 7.40 radians per second.

NACA-Langley - 12-19-52 - 1000